The Astrophysical Journal, 607:103–124, 2004 May 20

COMPARISON OF BAR STRENGTHS AND FRACTIONS OF BARS IN ACTIVE AND NONACTIVE GALAXIES

Eija Laurikainen and Heikki Salo
Division of Astronomy, Department of Physical Sciences, University of Oulu, Oulu FIN-90014, Finland; eija.laurikainen@oulu.fi

and

Ronald Buta
Department of Physics and Astronomy, Box 870324, University of Alabama, Tuscaloosa, AL 35487-0324
Received 2003 October 29; accepted 2004 February 6

ABSTRACT

Gravitational perturbation strengths and bar fractions in active and nonactive galaxies are compared using the Ohio State University Bright Galaxy Survey, which forms a statistically well defined sample of 180 disk galaxies. Bar fractions are studied using (1) the optical and near-IR classification of bars made by Eskridge and coworkers in 2002 and (2) our own bar classification based on Fourier decomposition of near-IR images (Fourier bars). The gravitational perturbation strengths are calculated using the bar torque method, taking the maximum ratio Q_g of the tangential force to the mean background radial force as a measure of the nonaxisymmetric perturbation. In addition, two-dimensional bulge-disk-bar decomposition is used to study the properties of bulges of the sample galaxies. In the near-IR, Seyfert galaxies, LINERs, and H II/starburst galaxies were found to have a similar fraction, 72%, of Fourier bars (or SB-type bars), compared to 55% in the nonactive galaxies. However, if SAB-type bars are also included, practically all (95%) H II/starburst galaxies have bars. In addition, a large fraction (34%) of bars in LINERs are obscured by dust in the optical region. We find that bars in early-type galaxies are at the same time long and massive and have weak perturbation strengths. Weak perturbation strengths can be explained by dilution of the nonaxisymmetric forces by the massive bulges: for a bulge-to-disk mass ratio B/D ranging from 0 to 1, the dilution may reduce Q_g from as high as 0.6 to as low as 0.1. On the other hand, bar length (relative to disk scale length) is not correlated with B/D, contrary to expectation. Seyfert- or LINER-type nuclear activity is present in most galaxies that have thin and thick planar bar components, whereas nuclear activity does not appear in those late-type galaxies that have extremely massive bars and strong perturbation strengths.

Subject headings: galaxies: active — galaxies: bulges — galaxies: evolution — galaxies: spiral — galaxies: statistics

1. INTRODUCTION

A large majority of galaxies show instabilities in their disks, which may affect evolution in their central regions. About 2/3 of disk galaxies are barred (Eskridge et al. 2000), and on scales smaller than 1 kpc more than half of them host secondary bars, central star clusters, spiral-like dust lanes, or star-forming rings (Carollo et al. 1997; Carollo, Stiavelli, & Mack 1998; Martini & Pogge 1999; Laine et al. 1999; Boker, Stanek, & Marel 2003). Nuclear spirals and dusty star-forming rings are associated with Seyfert galaxies and LINERs, whereas rings are typical in starburst galaxies of relatively early Hubble types. Many of these properties are dynamically linked to bars, which are efficient in triggering gas inflows in the disks (Shlosman, Begelman, & Frank 1990; Athanassoula 1992; Englmaier & Shlosman 2000) or collecting gas into resonance rings (Buta & Combes 1996 and references therein).

There is strong evidence for a connection between bars and nuclear starbursts, both theoretically and in terms of bar fractions showing that starburst galaxies are more often barred than nonactive systems (Ho, Filippenko, & Sargent 1997; Martinet & Friedli 1997; Hunt & Malkan 1999). In the linear theory of resonances, the inner Lindblad resonance is generally assumed to prevent the gas inflow to the very center. In many starburst galaxies, this resonance is manifested in the form of circumnuclear star-forming rings of kiloparsec scale. However, the connection is less clear for active galactic nuclei (AGNs), in which the activity is explained in terms of central black holes and their surrounding accretion disks, showing Seyfert- or LINER-type characteristics in the nearby universe. The conclusion from all the optical studies to date is that there is no difference in the fraction of bars between active and nonactive galaxies (Moles, Marquez, & Perez 1995; McLeod & Rieke 1995; Mulchaey & Regan 1997, hereafter MR97; Marquez et al. 2000; Ho et al. 1997; Hunt & Malkan 1999), although this is less clear in the near-IR, for which controversial results have been obtained (MR97; Knapen, Shlosman, & Peletier 2000, hereafter KSP00; Laine et al. 2002, hereafter LSKP02.

In the framework of the hierarchical dark matter cosmology, the formation and evolution of AGNs and their host galaxies are intimately related (Haehnelt, Natarajan, & Rees 1998; Fabian 1999; Mathur 2000), so that in order to evaluate the possible role of bars for the onset of nuclear activity, a comprehensive picture of galaxy evolution is needed. There is increasing evidence showing that supermassive black hole (SMBH) masses are correlated with the masses, luminosities, and velocity dispersions (Magorrian et al. 1998; Merritt & Ferrarese 2001) of bulges, which possibly indicates a close connection between their formation processes. SMBHs are probably formed soon after bulge formation and are relics of past quasar activity. In order to see present-day nuclear activity in these galaxies, fresh fuel is needed, as well as some driving

force, such as a bar, to transport the material toward the center. The feedback kinetic energy injected by jets or powerful winds of the SMBHs can be detected as heated X-ray atmospheres, but the outflowing energy is generally also visible in the optical region in the form of strong emission lines. Early-type spirals with massive bulges, and disks that still have a significant amount of gas are therefore expected to be favorable sites for Seyfert- and LINER-type nuclear activity.

However, galaxies are not dynamically passive, being continuously interacting with the intergalactic medium and with other galaxies, and bulges and disks are also dynamically coupled. For example, stellar disks can scatter stars originally in a bar to orbits above the plane of the disk into what resembles a bulgelike structure (Raha et al. 1991). In the presence of massive centrally peaked halos, the formed central concentrations can take boxy/peanut shapes (Athanassoula 2003), as is also observed in many galaxies (Lutticke, Dettmar, & Pohlen 2000). In fact, Bureau & Freeman (1999) have convincingly shown that boxy/peanut structures are bars seen edge-on. There are also other mechanisms such as resonance trapping (Quillen 2002) and chaotic diffusion (Combes et al. 1990; Pfenniger & Friedli 1991; Pfenniger & Norman 1990) that can produce similar boxy/peanut structures in galaxies. In this process the Hubble type can be changed toward an earlier morphological type (Pfenniger & Friedli 1991), suggesting that not all massive bulges were necessarily formed during the early epoch of galaxy formation and have old SMBHs.

Theoretical models predict that gas inflow is strongest in massive bars, when high-density shocks are present in the bar (Athanassoula 1992). Direct evidence of gas inflow for the SB(s)c spiral NGC 7479 has been found by Quillen et al. (1995), based on the kinematics of CO gas. The gas inflow is also sensitive to the effective sound speed of the gas, so that larger random motions favor a larger inflow rate (Englmaier & Gerhard 1997; Patsis & Athanassoula 2000). According to the models by Athanassoula (2003), bars that grow in halo/bulge-dominated disks are stronger than bars that grow in disk-dominated systems, which seems to explain the observation that bars are longer in early-type galaxies (Elmegreen & Elmegreen 1985). However, the connection between the mass of the bulge and the properties of the bars is not yet fully understood: for example, there is some evidence showing that bars in active galaxies, which are preferably early-type spirals, have *weaker* perturbation strengths than bars in late-type systems (Laurikainen, Salo, & Rautiainen 2002, hereafter LSR02).

In this paper we use the magnitude-limited sample of the Ohio State University Bright Galaxy Survey (OSUBGS; Eskridge et al. 2002, hereafter EFP02) to reinvestigate the perturbation strengths and bar fractions in active and nonactive galaxies. For this statistically well-defined sample, visual identifications of bars are available in both the optical and the near-IR, allowing a reliable comparison between the fractions of galaxies with bars in both wavelength regimes. The comparison is also made using bar identifications based on Fourier decompositions of disk density. The second part of this study is to compare bar-related gravitational perturbation strengths between active and nonactive galaxies and to investigate the role of bulges in controlling these properties. In both studies the OSUBGS sample is used, restricted in inclination and supplemented by a small set of nearby galaxies from the Two Micron All Sky Survey (2MASS; Skrutskie et al. 1997). As a measure of bar strength, forces are calculated from the *H*-band images, and the maximum ratio of the tangential force to the mean radial force is derived (Sanders & Tubbs 1980; Combes & Sanders 1981). This is a method that has become feasible only recently with the advent of near-IR imaging surveys (Buta & Block 2001, hereafter BB01). In addition, two-dimensional bulge-disk-bar decomposition is used for the same galaxies in order to estimate the scale and shape parameters of the bulges and to calculate bulge-to-disk (B/D) luminosity ratios. Our method used to calculate bar strengths has been greatly refined over previous studies and is described in detail by H. Salo, R. Buta, & E. Laurikainen (2004, in preparation). The measurements are provided by E. Laurikainen et al. (2004, in preparation).

2. THE SAMPLE

Our sample consists of 158 OSUBGS and 22 2MASS spirals. The sample is restricted to inclinations $\leq 65^\circ$ because deprojection of the galaxy images becomes more uncertain at higher inclinations. In addition to the inclination restriction, total magnitudes are restricted to $B_T < 12.0$, the Third Reference Catalogue of Bright Galaxies (de Vaucouleurs et al. 1991, hereafter RC3) type index is in the range $0 < T < 9$ (S0/a to Sm), and declinations are in the range $-80^\circ < \delta < +50^\circ$. In comparison to a distance-limited sample of 1264 galaxies from the catalog of Tully (1988), our sample is biased mainly against late-type, low-luminosity, barred spirals. The general properties of our sample are described in Buta, Laurikainen, & Salo (2004, hereafter BLS04).

Galaxies were divided into active and nonactive subsamples, based on the classifications given in the NASA/IPAC Extragalactic Database (NED), which mostly rely on spectral emission-line ratios (Veilleux & Osterbrock 1987): [O III] λ5007/Hβ, [N II] λ6583/Hα, [O II] λ3727/[O III] λ5007, and [O I] λ6300/[O III] λ5007. Seyfert galaxies have strong high-excitation emission lines, whereas LINERs also have prominent low-ionization lines. Galaxies with massive star formation in their nuclei are called H II/starburst galaxies, although only a few have nuclear starbursts with luminosities approaching those found in Seyfert galaxies and LINERs. In the following, Seyfert galaxies and LINERs together are called AGNs. The sample consists of 82 (46%) active galaxies, but after reassigning some of the intermediate types to main activity classes, the numbers add up to 102 cases (40 Seyfert, 38 LINER, and 24 H II/starburst). The number of H II/starburst galaxies in our sample is small compared to that found by Ho et al. (1997) for a magnitude-limited sample of galaxies. The most probable reason for this is that the spectroscopic study of Ho et al. was more sensitive to low-level nuclear activity. Using the classifications of RC3, the morphological types of Seyfert galaxies are found to be peaked at stage Sb ($\langle T \rangle = 3$), in agreement with Malkan, Gorjian, & Tam (1998). LINERs have morphological types fairly similar to those of Seyfert galaxies ($\langle T \rangle = 2.6$, Sab-Sb), whereas H II/starburst galaxies are more concentrated in later Hubble types ($\langle T \rangle = 4.2$, Sbc), in a manner similar to that of nonactive galaxies ($\langle T \rangle = 4.4$; see Fig. 1).

The mean morphological types (RC3 type index T), distances, radial scale lengths (h_r), and absolute blue magnitudes (M_B) for several subgroups of the galaxies are shown in Table 1. The *B*-magnitudes are from RC3, being corrected for Galactic extinction (Schlegel et al. 1998; taken from NED), and the distances (consistent with $H_0 = 75$ km s^{-1} Mpc^{-1}) from the catalog of Tully (1988). We generally used radial scale lengths measured from OSUBGS/2MASS images, but in some cases in which the *H*-band images were not deep

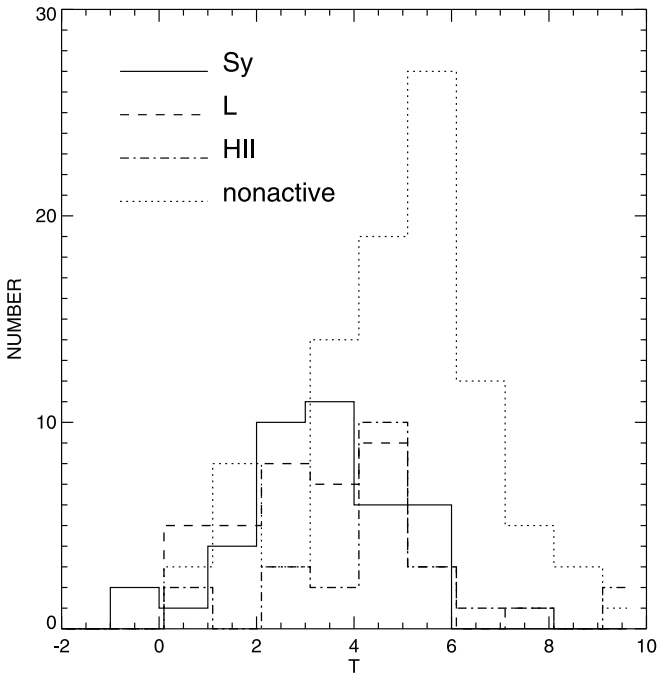

FIG. 1.—Histograms of the number of OSUBGS+2MASS sample galaxies, divided into active and nonactive galaxies, vs. RC3 type index. The activity types are taken from the NED.

enough, the scale lengths were taken from the literature. The early-type galaxies are on the average 0.2–0.35 mag more luminous, have 25% larger scale lengths, and appear at slightly larger distances than the late-type galaxies. This morphological segregation affects the properties of the Seyfert galaxies, LINERs, and H II/starburst galaxies. The H II/starburst galaxies, being associated mostly with late-type spirals, are generally smaller and dimmer than the Seyfert, LINER, and nonactive galaxies. Seyfert galaxies and LINERs, associated mainly with earlier type galaxies, are about 0.5 mag dimmer and 40% less distant than the early-type nonactive galaxies. In addition, as expected, active late-type galaxies are on the average slightly more distant, and consequently, because of the Malmquist bias the galaxies are slightly larger and brighter than the nonactive late-type systems. However, for the early-type galaxies the opposite seems to be true: among them, the nonactive galaxies are on average the more distant galaxies.

3. BAR FRACTIONS

3.1. *Bars in the Whole Sample*

Published classifications of bars represent mostly a visual exercise, and different observers may disagree on apparent bar strength. For example, in RC3 some galaxies are classified as SAB, even though the evidence for a bar is weak, while in the Revised Shapley-Ames Catalog (Sandage & Tammann 1981) and the Carnegie Atlas of Galaxies (Sandage & Bedke 1994), fairly obvious bars are sometimes not recognized. Thus, we must be cautious when comparing visual bar fractions between different studies, since the results may depend on the catalog used.

Using RC3 family classifications, our sample has an almost equal number of SA, SAB, and SB galaxies. Considering both SB and SAB types, $68\% \pm 4\%$ of the galaxies have bars, which is the same fraction as reported by EFP02 for the whole OSUBGS sample. This is also similar to that found by Moles et al. (1995) for a magnitude-limited sample of spirals (67% barred) and for normal galaxies selected by 12 μm flux by Hunt & Malkan (1999) (69% barred), but it is larger than that found by Sellwood & Wilkinson (1993) for field galaxies (60% barred) or by Ho et al. (1997) for a magnitude-limited sample of S0/a-Sm spirals (59% barred). We have traced the difference in the fraction of galaxies with bars between the Ho et al. (1997) sample and ours to two factors. First, these authors apparently counted as "nonbarred" 17 galaxies in their sample that had no family classification in RC3 (e.g., types such as .S..5..). If these cases are rejected, then the bar fraction in their sample increases to 62%. Second, they used no inclination restriction in computing their bar fraction, but for a fair comparison with our sample, we must make such a restriction. For the 228 spirals in the sample of Ho et al. with $\log R_{25} \leq 0.38$, the SAB+SB fraction is 64.5%. We conclude that our sample has a typical visual blue light bar fraction compared to other large samples of spiral galaxies, within the uncertainty of $\pm 4\%$.

The number of detected bars also depends on the wavelength, with many bars being more prominent in the near-IR than in blue light. This is due to the reduced effects of extinction and the greater prominence of the old stars in the near-IR. EFP02 used a conservative approach in classifying near-IR bars, but even so, 73% of the OSUBGS galaxies have bars in the near-IR, and 56% of them have apparently strong bars. However, as noted by BLS04, using near-IR images does not necessarily change the *rankings* of bars. A strong bar in blue

TABLE 1

MEAN PARAMETERS IN THE SUBSAMPLES

Sample	N	$\langle T \rangle$	$\langle M_B \rangle$	$\langle$Distance$\rangle$ (Mpc)	$\langle h_r \rangle$ (kpc)
All	180	3.8	−20.11	20.41	3.44 ± 2.19
Sy	40	3.0	−20.25	18.42	3.52 ± 2.27
LINER	38	2.6	−20.19	18.85	3.63 ± 1.77
H II/starburst	24	4.2	−19.82	19.57	3.03 ± 1.72
Nonactive	98	4.4	−20.10	21.28	3.49 ± 2.39
Early (T = 0–3)	76	1.9	−20.29	21.48	3.95 ± 2.54
Late (T = 4–9)	104	5.2	−19.94	19.63	3.06 ± 1.84
Active, early (Sy+LINER)	41	1.8	−20.16	18.24	3.50 ± 2.03
Nonactive, early	28	2.0	−20.64	26.87	4.82 ± 3.15
Active, late (Sy+LINER)	17	4.5	−20.44	21.87	3.76 ± 2.17
Nonactive, late	70	5.4	−19.88	19.04	2.96 ± 1.77

light may look even stronger in the near-IR, but there is no new bin in the classification system to recognize this.

In the near-IR, radial profiles of isophotal ellipticities and position angles were used by MR97, KSP00, and LSKP02 to identify bars. Taking into account the similarity of their methods, surprisingly different bar fractions were obtained (when restricted to control samples of normal galaxies): while MR97 found that 70% of their normal spirals have bars, KSP00 and LSKP02 found bar fractions of 59% and 50%, respectively. These differences are likely due to the degree to which the ellipticity profiles were relied on for recognizing bars. For example, MR97 recognized bars in some of their galaxies in the images, even though bars were not visible in the ellipticity profiles, whereas LSKP02 and KSP00 based all of their bar classifications strictly on ellipse fits. As discussed later, this difference is important to take into account when comparing the bar fractions these authors found in active and nonactive galaxies.

Given the occasional difficulty of interpreting ellipticity profiles, we prefer to use a Fourier method to unambiguously define bars in the H band (using the OSUBGS+2MASS sample). The main criteria are that strong $m = 2$ and 4 Fourier amplitudes be detected ($A_2/A_0 > 0.3$) and that their phases be maintained nearly constant in the bar region. We call bars identified in such a manner "Fourier bars." In our sample, 59% of the galaxies have Fourier bars (or 62% for $i < 60^\circ$). Because of the stringent definition, not all SAB-type bars are also Fourier bars. If we also include as barred galaxies systems classified as SAB by EFP02 in the H band, then 72% of the galaxies are barred, which is identical to the total number of bars (SB+SAB) reported by EFP02 for the OSUBGS sample.

3.2. *Bars in Active and Nonactive Galaxies*

The early study by Simkin, Su, & Schwarz (1980) singled out bars as important morphological components in Seyfert galaxies and LINERs, but the connection between bars and the presence of nuclear activity has turned out to be difficult to prove. Most surveys show no difference in the fraction of galaxies with bars between active and nonactive galaxies (McLeod & Rieke 1995; Moles et al. 1995; Ho et al. 1997; MR97; Hunt & Malkan 1999; Marquez et al. 2000), although the latest studies by KSP00 and LSKP02 have found a small excess of bars in Seyfert galaxies. Generally, sample biases or image resolution are suggested to explain these differences. In the following we argue that some real differences appear in the bar fractions between active and nonactive galaxies and that the most probable reason for the controversial earlier results is related to the wavelength and method used to identify bars.

Bar fractions were calculated in the optical using (1) the standard family classifications given in RC3, (2) bar classifications by EFP02 in the B band, (3) bar classifications by EFP02 in the H band, and (4) those made by us using the Fourier approach. For the statistical study of bar fractions, we use an inclination limit of 60°, less than our original limit of 65°. The reason for this is that bars are more difficult to recognize for inclinations larger than 60°, and we need to minimize this bias to get a reliable bar fraction (Laurikainen & Salo 2002, hereafter LS02). This new limit excludes 31 galaxies from the 180 galaxy sample. Galaxies were divided into subgroups according to morphological type and type of nuclear activity. If not specified otherwise, early types ($T = 0$–3) and late types ($T = 4$–9) refer to de Vaucouleurs' morphological types, coded on the RC3 numerical scale. In the H band the morphological types are generally shifted toward earlier types by 1 revised Hubble stage (EFP02). The bar fractions with associated uncertainties are shown in Table 2, where the variances are estimated from $\sigma^2 = [(1 - p)p]/N$ and p denotes the fraction of bars in a sample of N systems.

3.2.1. *Optical Bars*

Optical RC3 classifications, including both SB- and SAB-type bars, indicate that Seyfert galaxies and LINERs together have a bar fraction similar to that of nonactive systems (62% ± 7% vs. 69% ± 5% barred), a conclusion that is the same if the classifications of EFP02 are used (56% ± 7% vs. 57% ± 5% barred). In addition, the frequencies of SB-type bars in Seyfert galaxies and LINERs and in nonactive galaxies are very similar (34% ± 7% vs. 35% ± 5%). However, this kind of comparison overlooks some possibly real differences in the bar fractions between active and nonactive systems, because LINERs have a marginally lower fraction of optical bars than Seyfert galaxies in our small sample (EFP02; 46% ± 9% vs. 62% ± 9% barred).

In contrast, H II/starburst galaxies have optical bars marginally more frequently than nonactive systems (RC3: 78% ± 9% vs. 69% ± 5%; EFP02: 78% ± 9% vs. 57% ± 5% barred). The number of bars in H II/starburst galaxies evidently depends on the number of real starbursts in the sample. In their magnitude-limited sample of spiral galaxies, Ho et al. (1997) barely found an excess of bars in H II/starburst galaxies, whereas among the Markarian starburst galaxies, 87% of the galaxies are barred. Hunt & Malkan (1999) also report a high bar fraction of 82%–85% in their sample of star-forming galaxies.

3.2.2. *Bars in the Near-IR*

Near-IR imaging ought to provide a more reliable assessment of bar fractions. Bars are simply easier to detect in the near-IR, and we expect bar fractions to rise compared to the optical for this reason. Using the bar classifications of EFP02, the fraction of galaxies with bars in H II/starburst galaxies increases from 78% to 95% from the optical to the near-IR. For nonactive systems, which are peaked at late Hubble types, the number of galaxies with bars increases from 57% to 72%, and for Seyfert galaxies from 62% to 75%. However, for LINERs, which appear to have morphological types similar to those of Seyfert galaxies, the number of bars increases from 46% to 80%, indicating that the number of hidden bars in LINERs in the optical region is large. Considering all kinds of bars (SB+SAB) in the near-IR, the bar fraction in Seyfert galaxies is found to be similar to that in nonactive systems (75% ± 9% vs. 72% ± 4% barred). In LINERs, 80% ± 8% of the galaxies are barred, while almost all H II/starburst galaxies have bars (95% ± 5% barred).

We next compare these bar fractions with those obtained using the Fourier technique to identify bars in the near-IR. With these more objective classifications, Seyfert galaxies, LINERs, and H II/starburst systems have similar bar fractions: 69% ± 7%, 71% ± 8%, and 72% ± 10%, respectively. These are all higher than found for nonactive galaxies (55% ± 5% barred), indicating a statistically significant excess for Seyfert galaxies/LINERs, and a marginal excess for H II/starburst galaxies. This result is in contradiction to the bar fractions obtained using the classifications by EFP02 above, indicating again that the number of galaxies with bars depends on the

TABLE 2
FREQUENCY OF BARS

SAMPLE	SB+SAB, $i < 60^\circ$		SB, $i < 60^\circ$		SAB, $i < 60^\circ$		SB+SAB, $i < 65^\circ$	
	N_{bar}/N	Bar Fraction (%)	N_{bar}/N	Bar Fraction (%)	N_{bar}/N	Bar Fraction (%)	N_{bar}/N	Bar Fraction (%)
RC3								
Sy	18/29	62 ± 9	10/29	33 ± 9	8/29	28 ± 8	27/40	67 ± 7
LINER	16/28	57 ± 9	9/28	32 ± 9	7/28	25 ± 8	22/38	58 ± 8
H II/starburst	14/18	78 ± 9	6/18	33 ± 11	8/19	42 ± 11	17/24	71 ± 9
Sy+LINER	31/50	62 ± 7	15/50	30 ± 6	16/50	32 ± 6	43/67	64 ± 6
Nonactive	59/86	69 ± 5	32/86	37 ± 5	27/86	31 ± 5	66/98	67 ± 5
Early ($T = 0$–3)	33/51	65 ± 6	19/51	37 ± 7	14/51	27 ± 6	42/64	66 ± 6
Late ($T = 4$–9)	52/78	67 ± 5	23/78	29 ± 5	29/78	37 ± 5	58/89	65 ± 5
All	100/149	67 ± 4	52/149	35 ± 4	48/149	32 ± 4	120/180	67 ± 3
EFP02 (B Band)								
Sy	18/29	62 ± 9	9/29	31 ± 8	9/25	36 ± 9		
LINER	13/28	46 ± 9	11/28	39 ± 9	2/28	7 ± 5		
H II/starburst	14/18	78 ± 9	7/18	39 ± 11	7/18	39 ± 11		
Sy+LINER	28/50	56 ± 7	17/50	34 ± 7	11/50	22 ± 6		
Nonactive	49/86	57 ± 5	30/86	35 ± 5	19/86	22 ± 4		
Early ($T = 0$–3)	35/57	61 ± 6	21/57	37 ± 6	14/57	25 ± 6		
Late ($T = 4$–9)	42/70	60 ± 6	22/70	31 ± 5	20/70	29 ± 5		
All	88/140	63 ± 4	52/140	60 ± 4	36/140	26 ± 4		
EFP02 (H Band)								
Sy	18/24	75 ± 9	17/24	71 ± 9	1/24	4 ± 4		
LINER	20/25	80 ± 8	18/25	72 ± 9	2/25	8 ± 5		
H II/starburst	17/18	95 ± 5	12/18	67 ± 11	5/18	28 ± 10		
Sy+LINER	35/44	79 ± 6	32/44	72 ± 7	3/44	7 ± 4		
Nonactive	60/83	72 ± 4	48/83	58 ± 5	12/83	14 ± 4		
Early ($T = 0$–3)	60/84	71 ± 5	50/84	59 ± 5	10/84	12 ± 3		
Late ($T = 4$–9)	34/39	88 ± 5	23/39	59 ± 8	11/39	28 ± 7		
All	108/140	77 ± 3	89/140	64 ± 4	19/140	13 ± 3		
Fourier Bars (H Band), $i < 60^\circ$								
Sy	20/29	69 ± 7						
LINER	20/28	71 ± 8						
H II/starburst	13/18	72 ± 10						
Sy+LINER	36/50	72 ± 6						
Nonactive	47/86	55 ± 5						
All	93/149	62 ± 4						

method used to identify bars. The Fourier method largely picks up classical bars with prominent surface brightnesses, which is evidenced also by the fact that for Seyfert galaxies, LINERs, and H II/starburst galaxies, the relative fractions of SB-type bars ($71\% \pm 9\%$, $72\% \pm 9\%$, and $67\% \pm 11\%$) are similar to those obtained by the Fourier method.

The similar fractions of SB-type, near-IR bars and Fourier bars in the different activity types are not a morphological selection effect, because early- and late-type galaxies have similar fractions of SB-type bars (59% barred in the H band). Another possible bias is galaxy luminosity, because one would expect to see more bars in luminous galaxies, in which the disks are more reactive to bar formation because of the relatively lesser amount of halo component. However, the magnitude biases are small, so that they are not likely to play an important role in our conclusions: Seyfert galaxies are on the average 0.15 mag brighter, and LINERs only 0.09 mag brighter, than the nonactive galaxies in our sample. The bias is largest for H II/starburst galaxies, which are on the average 0.28 mag dimmer than nonactive systems, mainly because they also contain late-type dwarf galaxies.

There are three previous studies in the near-IR comparing bar fractions in active and nonactive galaxies: in two of them Seyfert galaxies were found to have bars more frequently than nonactive galaxies (KSP00: 79% vs. 59%; LSKP02: 73% vs. 50% barred), whereas MR97 detected similar bar fractions for Seyfert galaxies and for the comparison galaxies (70% barred). The results by KSP00 and LSKP02 are in good agreement with that found by us for SB-type bars and Fourier bars. Most likely, SB-type bar searches, Fourier bar searches, and searches using the ellipticity profiles all select similar bars. On the other hand, MR97 obtained a rather different result. Sample biases (magnitudes, distances) are not a plausible explanation, because MR97 matched their Seyfert and comparison samples in a manner similar to that of LSKP02. Since the bar fraction obtained by MR97 for Seyfert galaxies

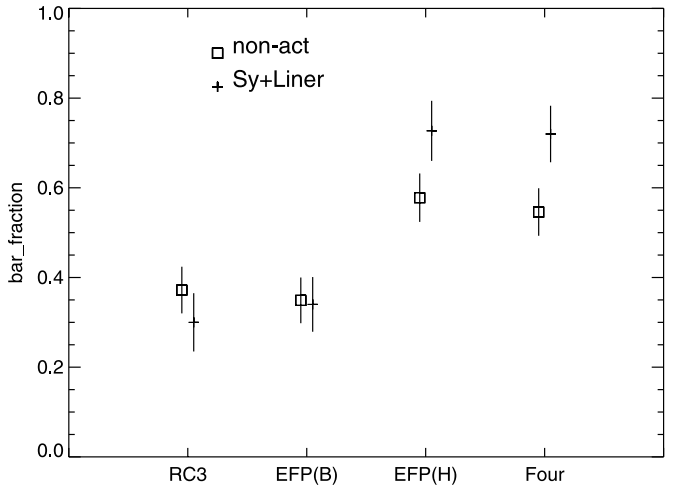

FIG. 2.—Fraction of SB-type bars in active and nonactive galaxies using the bar identifications given in RC3 and those made by EFP02 in the *B* and *H* bands (labeled "EFP [*B*]" and "EFP [*H*]," respectively). Bar frequencies using the Fourier technique to identify bars (labeled "Four") are also shown. The error bars indicate the mean errors for each subsample.

is similar to that in all the other studies in the near-IR, the key issue must be the comparison sample. Their way of identifying bars was mentioned above: by the additional visual identifications of bars, MR97 most probably added to barred galaxies a number of weak SAB-type bars, which for their lower surface brightnesses were overshadowed by prominent disks in the surface brightness profiles. From Table 2 we can see that SAB-type bars appear less frequently in Seyfert galaxies than in nonactive systems, which in principle could explain MR97's different result.

In conclusion, it seems that in the near-IR, which traces the mass distribution of disks better than the optical, all kinds of active galaxies have similar fractions of Fourier bars or SB-type bars, which is larger than in the nonactive galaxies. This difference from the nonactive galaxies is statistically significant for Seyfert galaxies and LINERs and marginally significant for H II/starburst galaxies. However, the total number of bars (SB+SAB) in H II/starburst galaxies is considerably higher than in Seyfert galaxies and LINERs mainly because they also have a large number of SAB-type bars, which are more rare in Seyfert galaxies and LINERs. The number of SAB-type bars is also large in the nonactive galaxies, which brings their total number of bars close to that found in Seyfert galaxies and LINERs. The main results are shown in Figure 2.

4. METHOD FOR ESTIMATING BAR STRENGTHS

The strength of a nonaxisymmetric perturbation is estimated by measuring the maximal ratio of the tangential force to the azimuthally averaged radial force, which is called the "gravitational torque method" (GTM; BB01). The gravitational potential is inferred from the two-dimensional *H*-band light distribution and is used to derive two-dimensional maps of radial (F_R) and tangential (F_T) forces, as well as a radial profile of the maximum relative tangential perturbation in each distance,

$$Q_T(r) = \frac{|F_T(r,\ \phi)|_{\max}}{\langle |F_R(r,\ \phi)| \rangle},$$

where $\langle |F_R(r,\ \phi)| \rangle$ denotes the azimuthally averaged axisymmetric force for each *r*. In constructing Q_T for each radius, we use the mean of the maxima over azimuth, calculated separately for the four image quadrants. The typical behavior of Q_T with radius is a rise to a maximum followed by a decline. This special force ratio maximum Q_g is then used as a single measure characterizing the strength of the nonaxisymmetric perturbation in a galaxy. Although Q_g is generally associated with a bar, in some cases, especially in SA galaxies, it may also be related to the spiral arms. If not otherwise noted, we use Q_g to indicate the maximum relative torque per unit mass per unit square of the circular speed, independent of whether it is associated with a bar or a spiral.[1] Another useful quantity is r_{Q_g}, which is the radial distance at which the maximum of Q_T occurs.

The main assumptions of our method are that the near-IR light distribution traces the mass, i.e., that the M/L ratio is constant and that the vertical density distribution can be represented by some simple function such as an exponential. The method is not sensitive to the form of the assumed vertical density distribution (LS02), but it is less clear whether all spiral galaxies have maximal disks. BLS04 used a statistical approach to calculate the effect of the dark matter halo on Q_g. In order to estimate the contribution of halos to radial forces, they used an empirical relation between galaxy luminosity and the halo density profile, which was derived by Persic, Salucci, & Stel (1996) from a large sample of rotation curves. The estimated uncertainty in Q_g was found to be 5% at maximum. Actually, a more important source of error on Q_g is the assumed vertical scale height, which may induce uncertainties of 10%–15%.

The GTM has been previously applied to large samples of galaxies by Block et al. (2001, 2002) and to a sample of 2MASS galaxies by LSR02 and LS02, who also refined the method. Instead of using a Cartesian grid for the evaluation of the potential (as in Quillen, Frogel, & Gonzalez 1994; Block et al. 2001, 2002), LSR02 and LS02 used a polar method, which is less sensitive to local pixel-to-pixel variations in the image. In addition, instead of using a single common value for the vertical scale height, h_z was estimated for each galaxy from the empirical relation between the radial exponential scale length and the vertical scale height, following de Grijs (1998). However, in all the above studies, large bulges were a problem because of artificial stretching of the bulge while deprojecting the images.

In this study we use the refined polar method (details in H. Salo et al. 2004, in preparation), in which the artificial stretching of the bulge is corrected. The bulge component is first separated using a two-dimensional bulge-disk-bar decomposition, where the bulge is described by a Sérsic model (Sérsic 1968) allowing for seeing effects, and the bulge and the disk are treated as in Möllenhoff & Heidt (2001). For the bar, a projected surface density distribution of a prolate Ferrers' bar with exponent 2 is used. The bulge model is then subtracted from the original image, the image is deprojected, and finally, the seeing-corrected bulge is added back by assuming that its luminosity is spherically distributed. The resulting bulge properties are not sensitive to the assumed bar model: the main purpose of explicitly including a bar in the decomposition is to insure that the bulge is not overestimated in the process. The

[1] The earlier studies by BB01, Block et al. (2001, 2002), LSR02, and LS02 all used the symbol Q_b for Q_g, as the method was originally intended to mainly highlight bar strength. Buta et al. (2003) recommended that Q_b should be used to strictly refer to a bar and discussed the separation of Q_g into bar and spiral (Q_s) components using Fourier methods.

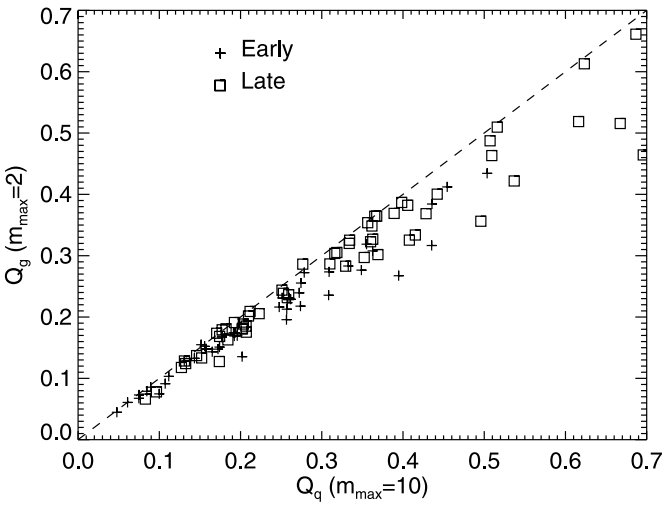

FIG. 3.—Comparison of relative maximum gravitational torques between when only the $m = 2$ Fourier amplitude of density is considered in the potential evaluation [$Q_g(m_{\max} = 2)$] and when all the even terms up to $m = 10$ are used [$Q_g(m_{\max} = 10)$]. The dependence is shown separately for early- and late-type spirals.

orientation parameters of the disks are derived from deep OSUBGS *B*-band images, and the vertical scale heights are estimated from the empirical relation between h_r/h_z and the RC3 type index T (de Grijs 1998), using the disk scale length derived from the decomposition in the *H* band. The measurements are described in E. Laurikainen et al. (2004, in preparation). Buta, Block, & Knapen (2003) have further developed the method by separating the contribution of spiral arms in the Q_T-profile, which might affect the bar torque measurements.

In this study we have used the even terms of $m = 2$–10 of the Fourier amplitudes of density to characterize the bars. However, as in some recent studies (Bournaud & Combes 2002; Block et al. 2002; Athanassoula 2003), we also consider only the $m = 2$ component. We checked how much the omission of the higher order terms could affect Q_g. Although Q_g ($m = 2$) is well correlated with Q_g ($m = 2$–10) (Fig. 3), it gives systematically lower gravitational perturbation strengths, in some cases underestimating them by as much as 30%.

5. INDEXES OF BAR STRENGTH IN ACTIVE AND NONACTIVE GALAXIES

Theoretical models (Athanassoula 2003) predict that when bars evolve in time, they transfer angular momentum to the halo and the bulge, and because of the associated slow-down of the pattern speed, bars become longer, more massive, and stronger. Indeed, in early-type galaxies where the bulges are generally massive, bars are also found to be longer (Elmegreen & Elmegreen 1985; Martin 1995) and to have stronger $m = 2$ density amplitudes (Athanassoula 2004) than in the late-type systems with less massive bulges. However, there is also growing evidence that bars in early-type systems have *weaker* gravitational perturbation strengths than bars in late-type systems (LSR02, BLS04). LSR02 also showed that bars are weaker in active than in nonactive systems, but the physical reason for that was not investigated. In the following we reinvestigate bar strengths in active and nonactive galaxies and discuss to what extent the Hubble type can explain the properties of bars. If not otherwise noted, in all the following by "barred galaxies" we mean systems for which bars were identified by the Fourier method.

5.1. *The Perturbation Strength, Q_g*

Figure 4 (*bottom*) shows the tendency for the $\langle Q_g \rangle$ of Fourier bars to increase from Sa ($T = 1$) toward later revised Hubble types, which has previously been shown for the whole OSUBGS sample by BLS04. The fact that our sample is biased against low surface brightness galaxies in principle might affect the type dependence of Q_g, because the low surface brightness galaxies are probably more dark matter–dominated. As noted by the referee, low surface brightness galaxies obey the Tully-Fisher relation and probably have a mass-to-light ratio dependent on surface brightness. Thus, M/L could vary systematically along the Hubble sequence. If the late-type galaxies in our sample are on average of lower surface brightness than the early-type galaxies, then our Q_g-values might be overestimated for the late-type galaxies because of this effect.

To investigate further the impact of surface brightness on our analysis, Figure 5 shows a plot of Q_g versus the mean surface brightness within the effective *B*-band isophote, estimated as (RC3)

$$\mu'_{e0} = m'_e - A_B(G) - 1.3(\log R_{25})^2,$$

where m'_e is the mean surface brightness within the photoelectrically determined effective aperture, $A_B(G)$ is the Galactic extinction, and R_{25} is the major-to-minor axis ratio of

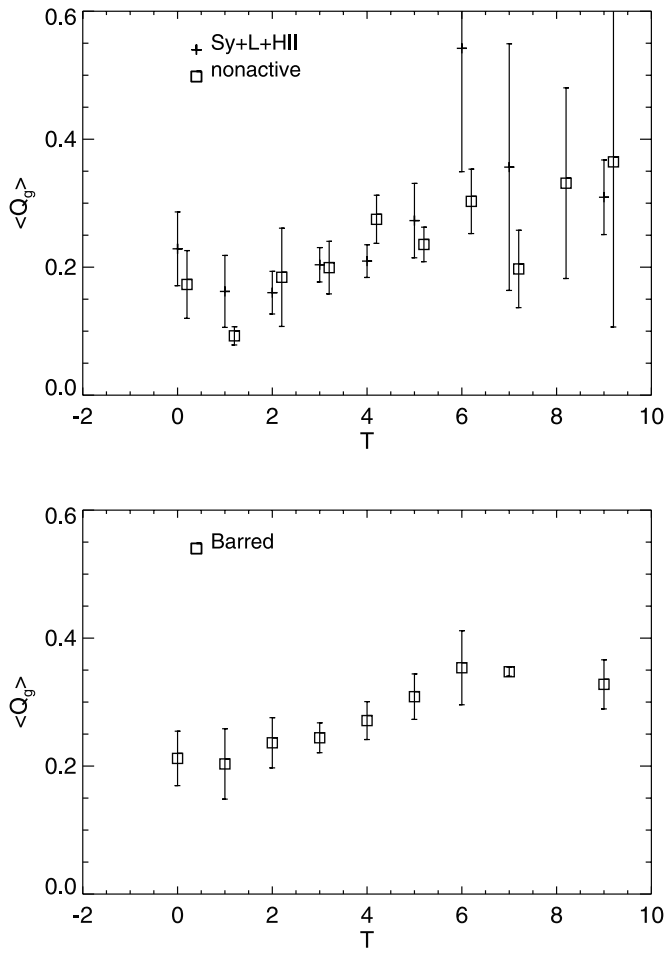

FIG. 4.—*Top*: Mean maximum relative torque Q_g vs. RC3 type index for active and nonactive galaxies. *Bottom*: Similar diagram for the barred galaxies in the sample, where bars are identified by the Fourier method. In this figure and in all the following figures, each activity type also includes the intermediate activity types. The error bars show the mean errors.

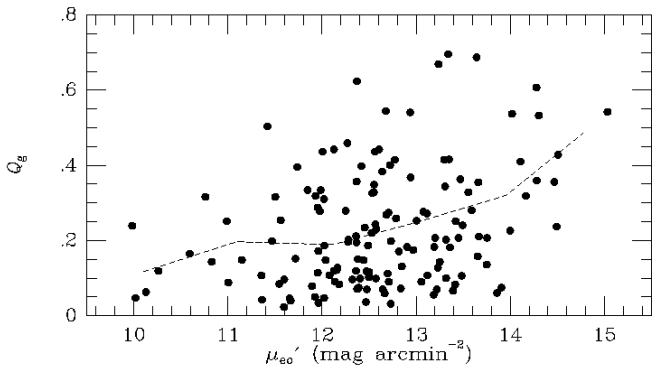

FIG. 5.—Plot of Q_g vs. mean surface brightness within the blue light effective isophote. The dashed line shows the averages of Q_g in 1 mag intervals.

the isophote having a B-band surface brightness of 25.00 mag arcsec^{-2} (all from RC3). The dashed line shows the averages of Q_g in 1 mag intervals. The figure shows that Q_g has some dependence on surface brightness in the sense that at higher surface brightnesses ($\mu_{e0}' < 13.0$ mag arcmin^{-2}), there is an upper envelope above which few galaxies are found, while at lower surface brightnesses, the selection criteria of our sample cause many low-luminosity, lower surface brightness galaxies (such as the "DDO dwarfs," which have surface brightnesses in the range of 13–17 mag arcmin^{-2}; de Vaucouleurs, de Vaucouleurs, & Buta 1981) to be excluded. The surface brightness effects are built into the type dependence we see in $\langle Q_g \rangle$, since mean effective surface brightness strongly depends on type (de Vaucouleurs & Buta 1983; Buta et al. 1994). Early-type spirals have a higher mean effective surface brightness on average, because of a greater bulge contribution on average. However, for our OSUBGS sample, BLS04 showed that typical corrections for dark matter are less than 10%. When dark halo–corrected values of Q_g are used, the type dependence of $\langle Q_g \rangle$ is only slightly affected (see Fig. 13 of BLS04). It is therefore unlikely that the type dependence of $\langle Q_g \rangle$ that we find can be fully accounted for by surface brightness bias. However, the issue merits giving special attention to bar strengths in low surface brightness giants and dwarfs.

We find a similar type dependence of Q_g for active and nonactive galaxies separately (Fig. 6), demonstrating that Seyfert galaxies and LINERs have small relative perturbation strengths, mainly because they appear in early Hubble types. Table 3 also shows that $\langle Q_g \rangle$ is similar for active and nonactive early-type galaxies. We can directly compare the mean bar torques of Seyfert galaxies, LINERs, and H II/starburst galaxies (from Table 3) with those estimated from Figure 4, based on their mean Hubble types: the mean type index $\langle T \rangle = 3.0$ for barred Seyfert galaxies corresponds to $\langle Q_g \rangle = 0.25$ for barred galaxies in Figure 4, which is very similar to the $\langle Q_g \rangle = 0.26 \pm 0.02$ calculated for Seyfert galaxies. Similarly, for H II/starburst galaxies the predicted and calculated values are $\langle Q_g \rangle = 0.28$ and 0.30 ± 0.03, respectively. For LINERs the mean type index $\langle T \rangle = 2.7$, and the calculated $\langle Q_g \rangle = 0.23 \pm 0.03$ are similar to the means for the Seyfert galaxies in Table 3.

In Figure 7 and Table 4 we show the mean radii at which the maximum Q_T occurs, normalized to the scale length of the disk (r_{Q_g}/h_r). In this case only barred galaxies are interesting, because the r_{Q_g} induced by spiral arms can appear almost anywhere in the disk. We examined the Q_T-profiles, and if the maximum was mainly associated with strong spiral arms, it was discarded from the analysis, which was the case for a few of the galaxies. The correlation of $\langle r_{Q_g}/h_r \rangle$ with the morphological type is opposite to that obtained for $\langle Q_g \rangle$: $\langle r_{Q_g}/h_r \rangle$ first slightly increases from S0/a ($T = 0$) to Sa types and then gradually decreases toward Scd types ($T = 6$). In addition, for galaxies earlier than Scd, active galaxies have systematically larger $\langle r_{Q_g}/h_r \rangle$-values than the nonactive systems of similar morphological types, although the error bars are large. This is in agreement with the earlier result by LSR02, who used a sample of 2MASS galaxies to show that $\langle r_{Q_g}/h_r \rangle$ is on the average larger for the active than for the nonactive galaxies.

The radius of the maximum Q_T is strongly correlated with the length of the bar, estimated by the Fourier method by assuming that bars have nearly constant phases of $m = 2$ and/or 4 density amplitudes: the coefficient of correlation is 0.94 (see Fig. 7, *top*). The maximum Q_T occurs on the average near the outer edge of the bar at a distance that is approximately 2/3 of the bar length (see, for example, Fig. 1 of BB01). This is in agreement with the simple models by LSR02 using the assumption that bars can be represented by Ferrer's potentials with a bar index $n = 2$. The correlation between r_{Q_g} and the length of a bar also means that bars are longer in early-type galaxies, in agreement with the previous results by Elmegreen & Elmegreen (1985) and Martin (1995). In addition, bars are long in Seyfert galaxies and LINERs, which are preferentially early-type systems.

Early-type bars are known to have flatter intensity profiles than late-type bars (Elmegreen & Elmegreen 1985), which in principle could affect r_{Q_g}. In Figure 7 (*bottom*) are shown the mean r_{Q_g}-values, normalized to the length of a bar, for each Hubble type. There is a tendency for galaxies earlier than Scd to have r_{Q_g} located more toward the end of a bar than for the later type galaxies. Within the error bars, active and nonactive galaxies have quite similar $\langle r_{Q_g}/r_{\rm bar} \rangle$-values. However, early-type active galaxies have $\langle r_{Q_g}/r_{\rm bar} \rangle = 0.79 \pm 0.061$, which is larger than the 0.69 ± 0.03 found for the nonactive early-type galaxies (see Table 5) (if H II/starburst galaxies are excluded, $\langle r_{Q_g}/r_{\rm bar} \rangle = 0.82 \pm 0.06$). This probably means that bars in active early-type galaxies have on average flatter

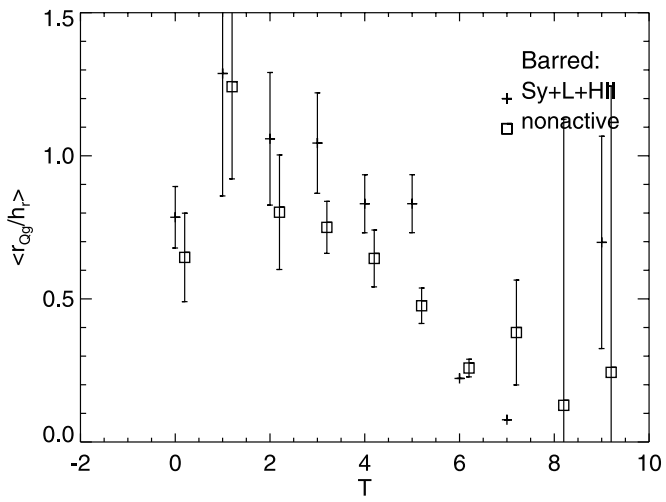

FIG. 6.—Mean distances of the maximum Q_T-values relative to the radial scale length vs. the RC3 type index, shown for barred active and barred nonactive galaxies. The points with no error bars are based on 1 galaxy only. The Q_T-profiles were first inspected, and only bar-induced tangential forces were taken into account. However, no bar/spiral separation was applied to the Q_T-profiles.

TABLE 3
MEAN Q_g

SAMPLE	ALL GALAXIES		BARRED	
	$\langle Q_g \rangle \pm$ Mean Error	N	$\langle Q_g \rangle \pm$ Mean Error	N
Sy+LINER+H II	0.211 ± 0.015	82	0.252 ± 0.019	54
Sy+LINER	0.191 ± 0.017	58	0.235 ± 0.021	43
Sy	0.206 ± 0.022	40	0.250 ± 0.029	25
LINER	0.176 ± 0.023	38	0.231 ± 0.033	23
H II/starburst	0.261 ± 0.029	24	0.298 ± 0.036	16
Nonactive	0.231 ± 0.015	98	0.267 ± 0.033	50
Early ($T = 0$–3)	0.178 ± 0.015	74	0.225 ± 0.017	47
Late ($T = 4$–9)	0.258 ± 0.015	101	0.288 ± 0.031	57
Active, early (Sy+LINER+H II)	0.187 ± 0.019	46	0.227 ± 0.023	32
Active, early (Sy+LINER)	0.171 ± 0.018	39	0.213 ± 0.021	28
Nonactive, early	0.164 ± 0.024	28	0.221 ± 0.026	15
Active, late (Sy+LINER+H II)	0.243 ± 0.028	31	0.288 ± 0.034	22
Active, late (Sy+LINER)	0.246 ± 0.027	32	0.277 ± 0.044	15
Nonactive, late	0.262 ± 0.019	67	0.287 ± 0.046	35
Region I			0.241 ± 0.013	65
Region II			0.398 ± 0.078	20

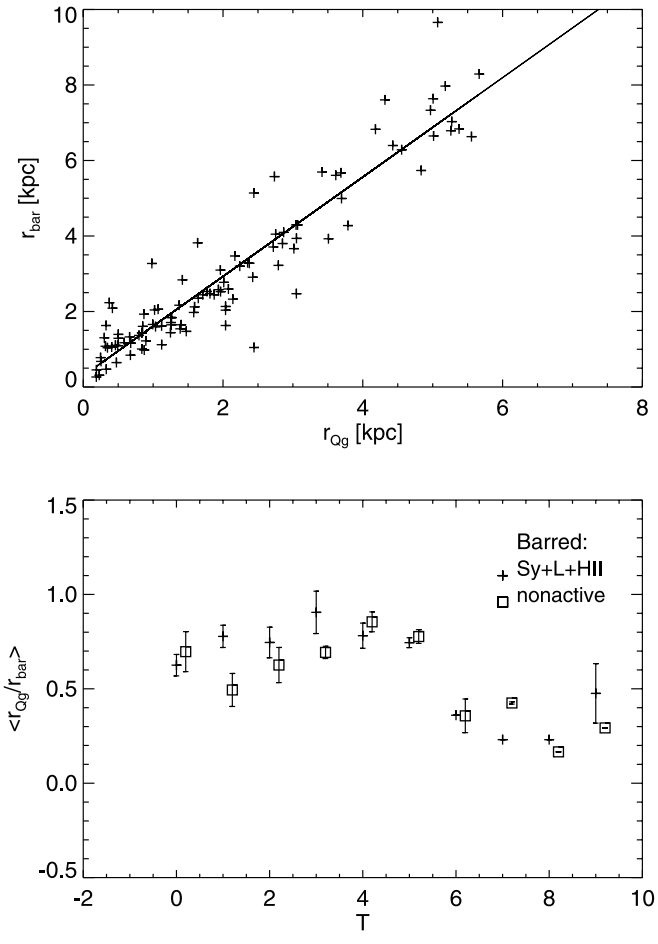

FIG. 7.—*Top*: Correlation between the length of the bar and the radius of the Q_T-maximum. The length of the bar is estimated from the $m = 2$ and 4 Fourier phases by assuming that they are maintained nearly constant in the bar region. The line shows a least-squares fit slope of 1.3 between the two parameters (the coefficient of correlation is 0.94). *Bottom*: Ratio $r_{Q_g}/r_{\rm bar}$ as a function of RC3 type index T for barred active (Seyfert+LINER+H II) and nonactive galaxies.

surface brightness distributions than bars in their nonactive counterparts.

5.2. $m = 2$ *Density Amplitudes,* A_2

We have shown that Q_g and r_{Q_g}/h_r have opposite correlations with Hubble type. However, neither of these parameters can be directly tied to the mass of a bar. Both parameters are affected by massive bulges, which dilute Q_g and push r_{Q_g} outward. A better estimate of the relative mass of a bar is the Fourier amplitude of density: when normalized to the $m = 0$ component, the underlying disk and bulge are taken into account. We use the $m = 2$ (A_2) and $m = 4$ (A_4) components, which are the dominant modes in bars and have the advantage of appearing above the noise level for all barred galaxies.

In order to avoid noise, especially in the outer parts of the images, and also to avoid strong $m = 2$ amplitudes induced by strong spiral arms, we did not automatically select the maximum amplitude of density over all radii. Instead, Q_T-profiles were first inspected, and the distance of the maximum Q_T, corresponding to a bar, was found. Then the radial profiles of the density amplitudes were investigated near that distance, within 15 pixels inward and 35 pixels outward from the Q_T maximum. This procedure facilitated the selection of only those amplitude peaks that are associated with the bar. We found that both $\langle A_2 \rangle$ and $\langle A_4 \rangle$ are more pronounced in early-type galaxies and *decrease* toward later types (Fig. 8, *top left*). Using the same amplitudes for the potential evaluation of bars, the mean Q_g was found to *increase* toward later Hubble types (Fig. 8, *top right*), as was also the case when higher Fourier terms were taken into account (see Fig. 4). At first sight, this is surprising because Q_g increases with the increasing density amplitude, as is also shown in Figure 8 (*bottom*). However, the correlation is more shallow for early-type galaxies, so that for a certain Q_g, the early-type galaxies have stronger $m = 2$ amplitudes than the late-type systems. This is one of the most important results of this paper, and it clearly indicates that *bars in early-type galaxies can at the same time be massive and have weak perturbation strengths*. Since strong perturbation strength also means high ellipticity of a bar (LSR02, BLS04), our result challenges the evolutionary picture of bars as outlined by Athanassoula (2003). The derived correlations

TABLE 4
MEAN r_{Q_g}/h_R

SAMPLE	ALL GALAXIES		BARRED	
	$\langle r_{Q_g}/h_r\rangle \pm$ Mean Error	N	$\langle r_{Q_g}/h_r\rangle \pm$ Mean Error	N
Sy+LINER+H II	1.046 ± 0.070	82	0.854 ± 0.064	48
Sy+LINER	1.114 ± 0.088	58	0.888 ± 0.075	37
Sy	1.168 ± 0.114	40	0.984 ± 0.123	20
LINER	1.028 ± 0.108	38	0.775 ± 0.063	22
H II/starburst	0.880 ± 0.104	24	0.685 ± 0.091	16
Nonactive	0.847 ± 0.058	98	0.552 ± 0.049	44
Early (T = 0–3)	1.038 ± 0.073	74	0.907 ± 0.069	39
Late (T = 4–9)	0.857 ± 0.056	101	0.567 ± 0.044	57
Active, early (Sy+LINER+H II)	1.102 ± 0.101	46	0.930 ± 0.093	27
Active, early (Sy+LINER)	1.159 ± 0.115	39	0.959 ± 0.108	23
Nonactive, early	0.933 ± 0.099	28	0.855 ± 0.088	12
Active, late (Sy+LINER+H II)	1.051 ± 0.100	31	0.757 ± 0.080	21
Active, late (Sy+LINER)	1.021 ± 0.102	32	0.770 ± 0.096	14
Nonactive, late	0.802 ± 0.073	58	0.439 ± 0.045	32
Region I			0.780 ± 0.037	65
Region II			0.374 ± 0.058	20

also explain why Seyfert galaxies and LINERs, appearing preferentially in early-type systems, have on average more massive bars and relatively weaker gravitational perturbation strengths than the nonactive systems, whereas H II/starburst galaxies, appearing preferentially in later type systems, have stronger gravitational perturbations (see Tables 3 and 6).

5.3. *Comparison of Different Indexes of Bar Strength*

In § 3 we used the family classifications of EFP02 in the near-IR to study bar fractions in active and nonactive galaxies. We found that all active galaxy classes (Seyfert galaxies, LINERs, and H II/starburst galaxies) have similar fractions of SB-type bars (or Fourier bars), which are generally thought to be strong bars. In the following we discuss whether this also means that Seyfert galaxies, LINERs, and H II/starburst galaxies have similar fractions of *massive* bars.

In Figure 9 we show how the family classes in the near-IR are related to the above discussed parameters characterizing the prominence of bars. In spite of the large overlap between SB- and SAB-type galaxies, it is also clear that SB-type bars have on the average stronger density contrasts (A_2) and perturbation strengths (Q_g) than SAB-type bars. On the other hand, we also showed previously that bars are more massive in early-type galaxies (or in Seyfert galaxies and LINERs; Fig. 8). Therefore, it is possible that H II/starburst galaxies (appearing in late-type systems) have *more* SB-type bars than do Seyfert galaxies and LINERs because, given the smaller masses of their bars, not all bars were detected. However, A_2 and A_4 amplitudes for H II/starburst galaxies are not significantly smaller than for Seyfert galaxies or LINERs (Table 6), so our conclusion is that Seyfert galaxies, LINERs, and H II/starburst galaxies have similar fractions of massive bars.

Another finding in § 3 was that the total number of bars in H II/starburst galaxies is extremely high, mainly because, in addition to SB-type bars, they also have a large number of SAB-type bars. An interesting question is then what makes SAB-type bars favorable for strong nuclear/circumnuclear star formation but not for Seyfert- or LINER-type nuclear activity?

On the basis of our data alone, it is difficult to explain this, but we can learn something by comparing the histograms of

TABLE 5
MEAN SCALED BAR LENGTHS AND r_{Q_g}-VALUES

Sample	$\langle r_{\rm bar}/h_r\rangle$	N	$\langle r_{Q_g}/r_{\rm bar}\rangle$	N
Sy+LINER+H II	1.217 ± 0.090	48	0.754 ± 0.039	54
Sy+LINER	1.218 ± 0.107	37	0.787 ± 0.045	43
Sy	1.336 ± 0.180	20	0.842 ± 0.068	25
LINER	1.074 ± 0.080	22	0.715 ± 0.039	23
H II/starburst	1.087 ± 0.131	16	0.633 ± 0.058	16
Nonactive	0.919 ± 0.064	44	0.602 ± 0.027	50
Early (T = 0–3)	1.303 ± 0.104	39	0.759 ± 0.040	47
Late (T = 4–9)	0.907 ± 0.056	53	0.616 ± 0.030	57
Active, early (Sy+LINER+H II)	1.300 ± 0.138	27	0.792 ± 0.057	32
Active, early (Sy+LINER)	1.292 ± 0.154	23	0.816 ± 0.061	28
Nonactive, early	1.307 ± 0.139	12	0.690 ± 0.029	15
Active, late (Sy+LINER+H II)	1.109 ± 0.103	21	0.698 ± 0.049	22
Active, late (Sy+LINER)	1.096 ± 0.129	14	0.731 ± 0.060	15
Nonactive, late	0.774 ± 0.052	32	0.565 ± 0.036	35
Region I	1.075 ± 0.052	65	0.754 ± 0.032	65
Region II	0.808 ± 0.079	20	0.453 ± 0.043	20

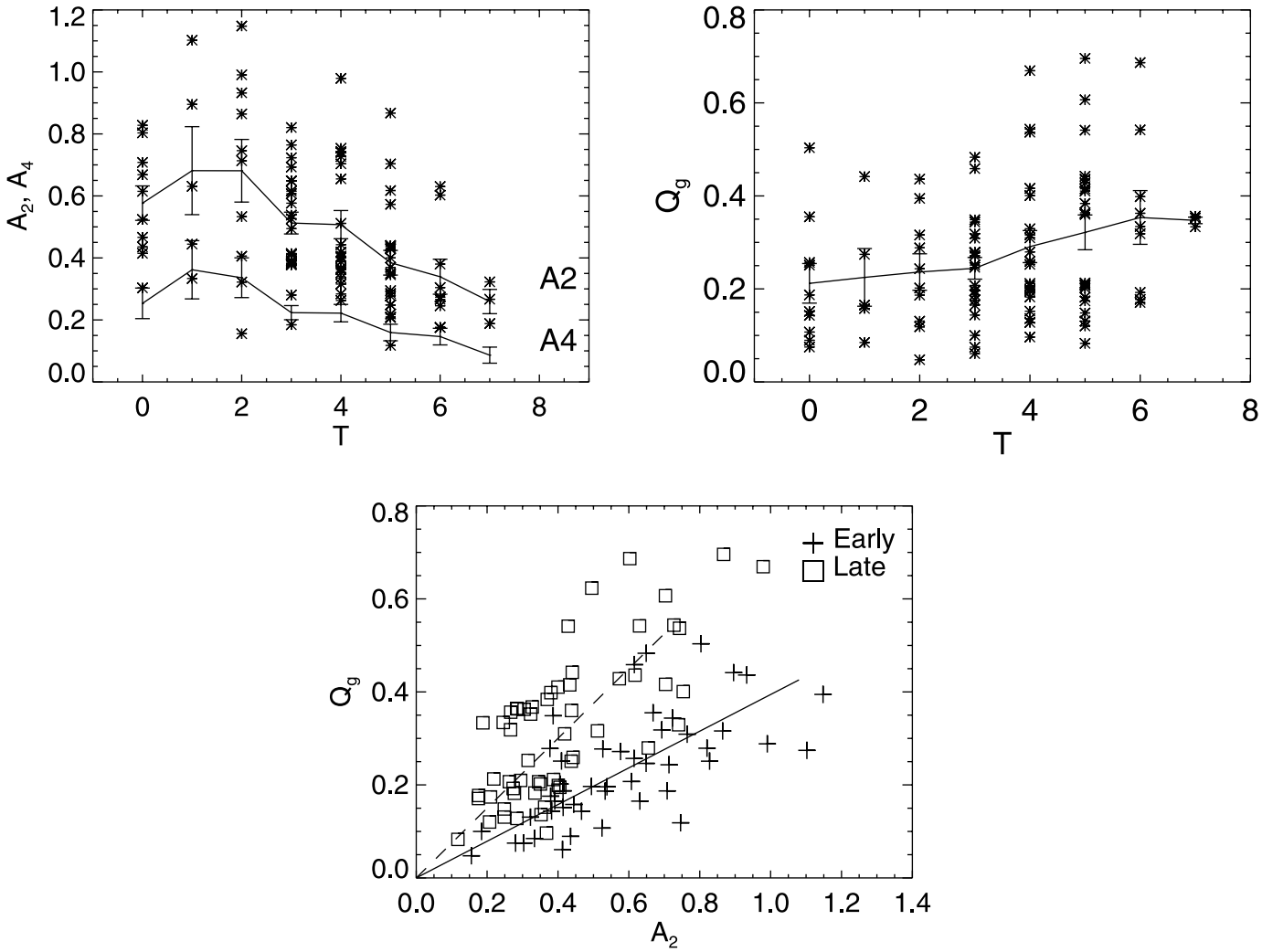

FIG. 8.—*Top left*: Plot of the $m = 2$ and 4 amplitude of density (A_2 and A_4) vs. RC3 type index for the sample galaxies. The measurements are shown only for $m = 2$, and the lines show the mean values of A_2 and A_4 assigned to each Hubble type. *Top right*: Maximum gravitational perturbation strength vs. RC3 type index when only $m = 2$ amplitudes of density are considered in the potential evaluation. *Bottom*: Maximum perturbation strength vs. the amplitude of density when only the $m = 2$ mode is considered, showing early- and late-type galaxies separately.

TABLE 6

MEAN A_2 AND A_4 FOR BARRED GALAXIES

Sample	$\langle A_2 \rangle \pm$ Mean Error	N	$\langle A_4 \rangle \pm$ Mean Error
Sy+LINER+H II	0.532 ± 0.033	54	0.244 ± 0.023
Sy+LINER	0.541 ± 0.036	43	0.255 ± 0.026
Sy	0.564 ± 0.046	25	0.260 ± 0.032
LINER	0.511 ± 0.053	23	0.252 ± 0.039
H II/starburst	0.505 ± 0.069	16	0.219 ± 0.046
Nonactive	0.442 ± 0.028	50	0.184 ± 0.016
Early ($T = 0$–3)	0.580 ± 0.034	47	0.269 ± 0.023
Late ($T = 4$–9)	0.414 ± 0.025	57	0.172 ± 0.015
Active, early (Sy+LINER+H II)	0.588 ± 0.046	32	0.276 ± 0.031
Active, early (Sy+LINER)	0.579 ± 0.048	28	0.273 ± 0.034
Nonactive, early	0.563 ± 0.039	15	0.252 ± 0.027
Active, late (Sy+LINER+H II)	0.451 ± 0.039	22	0.198 ± 0.029
Active, late (Sy+LINER)	0.470 ± 0.051	15	0.221 ± 0.039
Nonactive, late	0.390 ± 0.033	35	0.155 ± 0.017
Region I	0.508 ± 0.028	65	0.222 ± 0.019
Region II	0.515 ± 0.053	20	0.238 ± 0.031

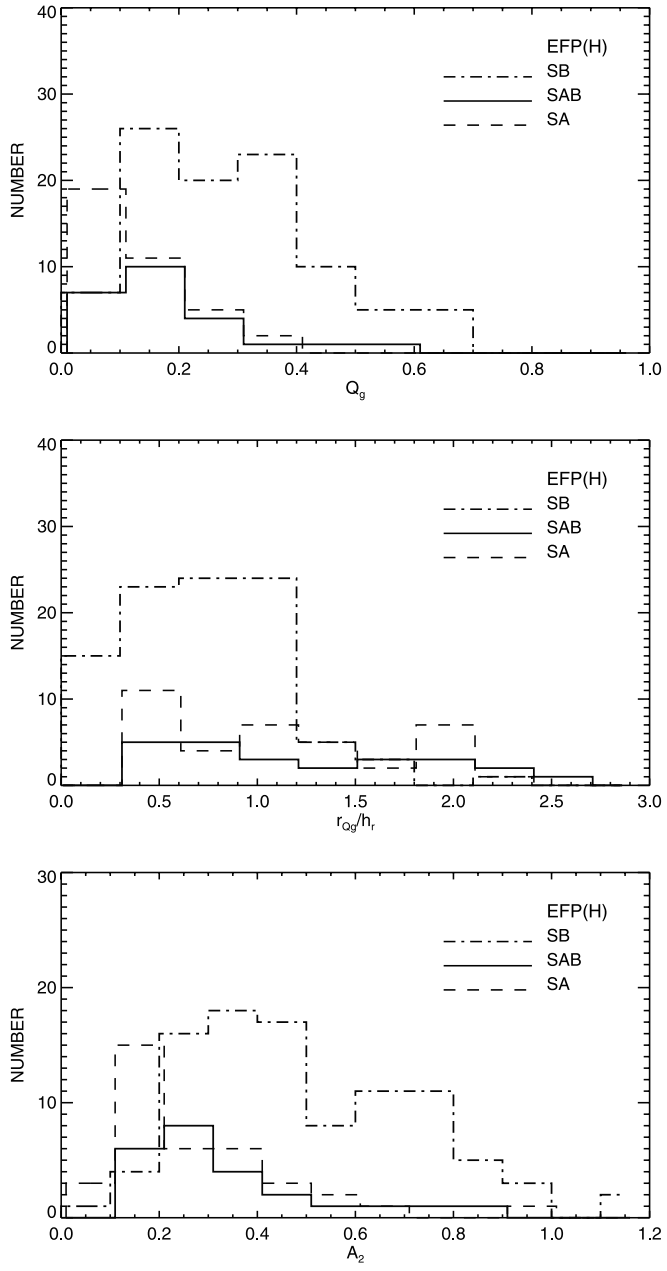

FIG. 9.—Histograms of the number of sample galaxies vs. the maximum relative gravitational torque (Q_g), the radius of this maximum scaled to the scale length of the disk (r_{Q_g}/h_r), and the $m = 2$ amplitude of density (A_2). For all three parameters the de Vaucouleurs' family classes by EFP02 in the H band are shown.

the number of sample galaxies with the three parameters of the bars, Q_g, r_{Q_g}/h_r, and A_2. As expected, SAB-type bars both are less massive and have on the average weaker perturbation strengths than SB-type bars: except for a few galaxies, SAB-type bars represent the lower end in the distribution of SB-type bars for both parameters. SAB-type galaxies also largely overlap with the nonbarred SA-type galaxies, whereas for the optically identified bars, the overlap is considerably smaller (see BB01). Most interesting is perhaps what is shown in Figure 9 (*middle*): although the perturbation strengths of SAB-type galaxies are small, their r_{Q_g}/h_r-values are large. This probably means either that they have flatter bars or, alternatively, that the bars are longer than in SB-type galaxies, which is not intuitively expected.

6. BULGES IN ACTIVE AND NONACTIVE GALAXIES

Above we have discussed the parameters Q_g, r_{Q_g}/h_r, and A_2 in active and nonactive galaxies, showing that if bars are long and have strong density contrasts (are massive), it does not necessarily mean that they also have strong perturbation strengths. However, all these parameters are correlated with the morphological type, which implies that bulges most probably play an important role in controlling them. In the following we use two-dimensional bulge-disk-bar decomposition to study the scale parameters and bulge-to-disk luminosity ratios (B/D) for the same galaxies.

We use the generalized Sérsic (1968) radial intensity profile to represent the bulge:

$$I(r) = I_e \exp\left\{-b_n\left[(r/r_e)^{1/n} - 1\right]\right\},$$

where I_e is the intensity at the effective radius r_e, which encloses 50% of the light. The parameter n is a shape parameter, so that large n-values correspond to more peaked surface brightness distributions. Values of $n = 1$ and 4 are special cases of the more general function, so that $n = 1$ corresponds to an exponential distribution and $n = 4$ to the $R^{1/4}$ law. In principle, a good approximation is available for calculating b_n for $n = 1$–10, but since many of the galaxies in our sample have $n < 1$, the exact expression for b_n was used to calculate r_e (Graham 2001). The B/D ratio was calculated including in the disk both the exponential disk and the bar; thus, the adopted bar model is not critical for the derived B/D ratio. In the statistical analysis, using the decomposition results, we eliminated nine galaxies for which the decomposition was uncertain, either because the images were not deep enough or because the bulge was too poorly resolved from the underlying bright disk.

6.1. *B/D Ratio versus the Indexes of Bar Strength*

In Figure 10 we show Q_g versus the B/D ratio for all galaxies in the sample. The plot shows that Q_g for a given B/D ratio gradually decreases toward larger B/D ratios. This B/D-dependent upper limit is a clear manifestation of the fact that massive bulges, which form an important part of the axisymmetric component, dilute the nonaxisymmetric gravitational forces. If all the weakening of Q_g is assumed to be due to the dilution effect, Q_g can be reduced from as much as $\sim$0.6 to as little as 0.1, corresponding to five bar torque classes as defined by BB01. Similar diagrams, divided into early/late and active/nonactive galaxies, are shown in Figure 11. A logarithmic scale is used in order to better show the galaxies with small B/D ratios. The dilution starts to be visible already for $B/D > 0.1$. Since the large majority of early-type galaxies have massive bulges, the dilution effect is a plausible explanation for their weak perturbation strengths. On the other hand, bars in late-type galaxies, where the bulges are less massive, are not much affected. This is also an obvious reason why H II/starburst galaxies can have strong perturbation strengths. The correlations of r_{Q_g}/h_r and A_2 with the B/D ratio are shown in Figures 12 and 13. Although the perturbation strength is largely controlled by the bulge mass, the effect of the bulge is less important for r_{Q_g}/h_r, which for most of the early-type galaxies is nearly constant. Late-type galaxies have smaller r_{Q_g}/h_r-values than the early-type systems, but again, the length of a bar does not depend on the B/D ratio; r_{Q_g}/h_r is small for all galaxies with $B/D < 0.03$, but it is also small for many late-type galaxies with massive bulges.

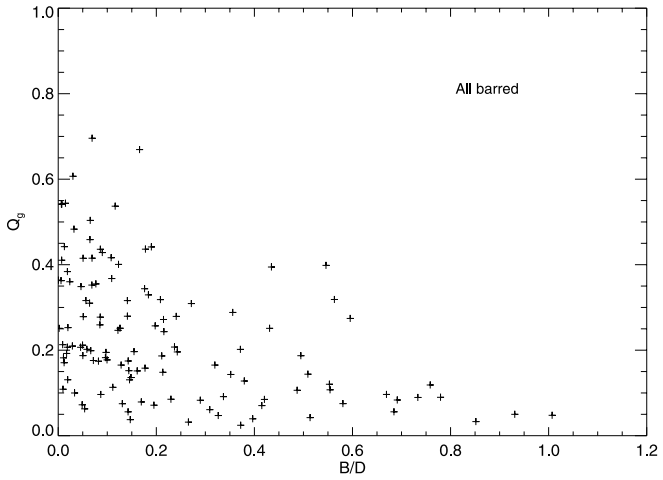

FIG. 10.—Maximum relative gravitational torque (Q_g) vs. bulge-to-disk (B/D) mass ratio for the barred galaxies in the sample. The linear scale shows well how massive bulges dilute the nonaxisymmetric perturbations in bars.

There is some evidence showing that the upper limit of the density contrast, A_2, increases toward larger B/D ratios (Fig. 13), which is in line with the predictions of the models by Athanassoula (2003). However, the tendency is weak, and actually, a more significant characteristic in the diagram is that early-type galaxies have on average stronger density contrasts

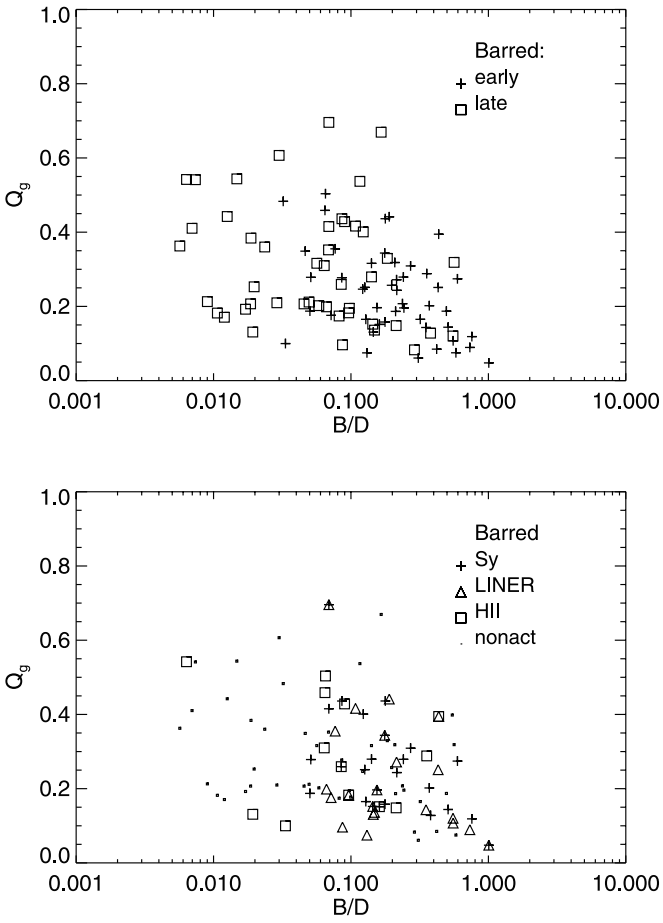

FIG. 11.—Maximum relative gravitational torque (Q_g) vs. B/D ratio. *Top*: Barred early- ($T = 0$–3) and late-type ($T = 4$–9) spirals, based on the morphological classifications in RC3. *Bottom*: Barred active and nonactive galaxies.

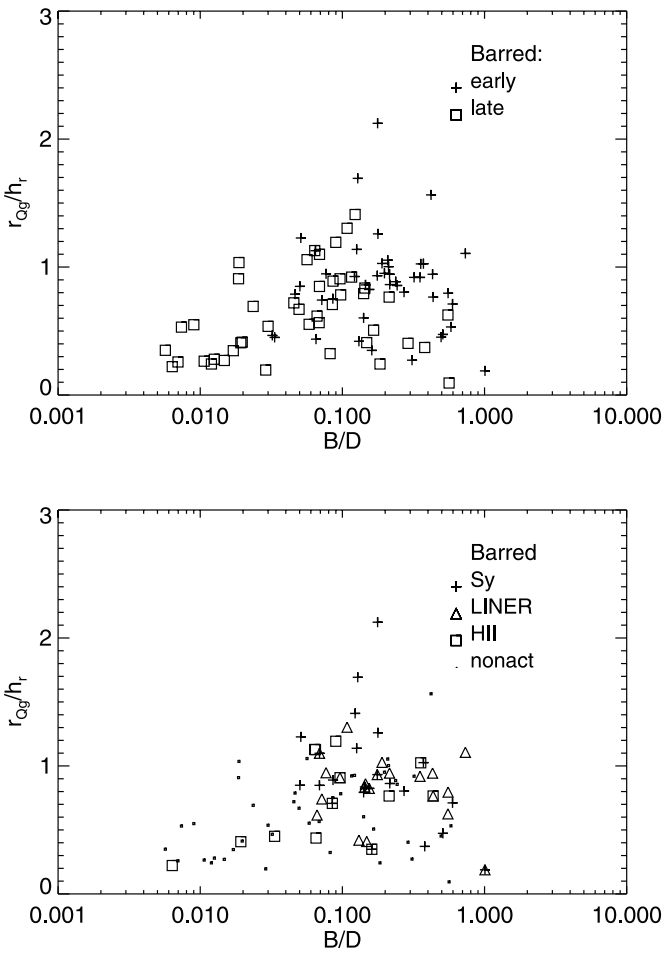

FIG. 12.—Distance of the maximum Q_T scaled to the scale length of the disk (r_{Q_g}/h_r) vs. B/D ratio. *Top*: Barred early- ($T = 0$–3) and late-type ($T = 4$–9) spirals, based on the morphological classifications in RC3. *Bottom*: Barred active and nonactive galaxies.

than the late-type systems. Seyfert galaxies and LINERs have a large scatter in the diagram, but they behave largely in a manner similar to that of the early-type galaxies. In addition, H II/starburst galaxies do not appear preferentially in late-type galaxies with $B/D < 0.05$.

In order to have a direct comparison with the models by Athanassoula (2003), we also calculated the corresponding density parameter S_b:

$$S_b = \frac{\int_0^{R_{\max}} \sqrt{A_m^2 + B_m^2}\, r\, dr}{\int_0^{R_{\max}} A_0 r\, dr},$$

where

$$A_m(r) = \frac{1}{\pi} \int_0^{2\pi} \sigma(r,\ \Theta) \cos(m,\ \Theta)\, d\Theta,$$

$$B_m(r) = \frac{1}{\pi} \int_0^{2\pi} \sigma(r,\ \Theta) \sin(m,\ \Theta)\, d\Theta,$$

and $\sigma(r,\ \Theta)$ is the projected surface density. In the calculation we extended these formulas for a single Fourier component to cover all even terms up to $m = 10$, by taking into account the amplitudes and phases of the different m-components. This is an alternative way of estimating the density amplitudes of

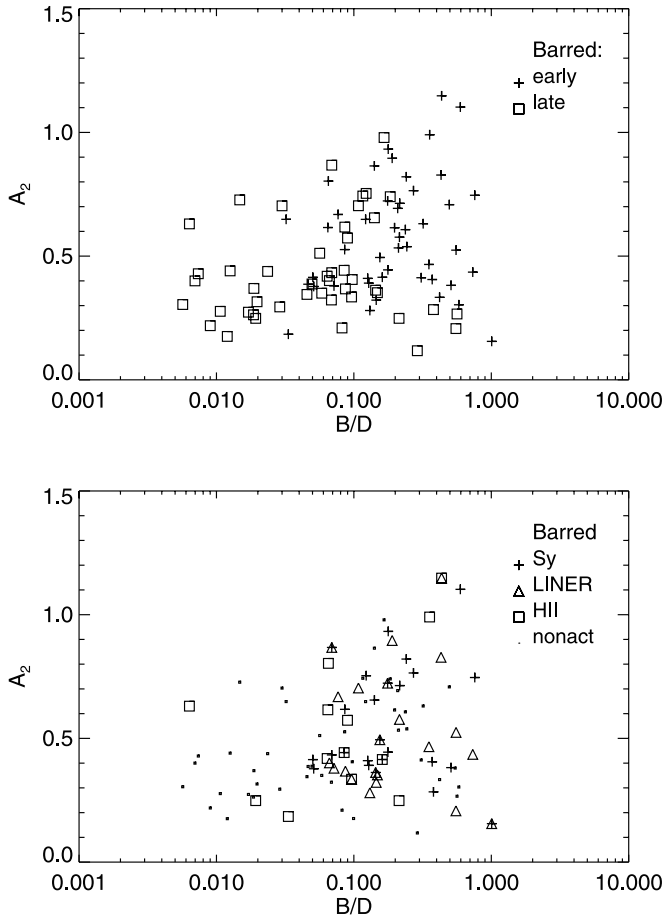

FIG. 13.—Plot of the $m = 2$ amplitude of density (A_2) vs. B/D ratio. *Top*: Barred early- ($T = 0$–3) and late-type ($T = 4$–9) spirals, based on the morphological classifications in RC3. *Bottom*: Barred active and nonactive galaxies.

bars, and therefore it is not unexpected that the correlation of S_b with the B/D ratio (Fig. 14) is quite similar to that for A_2: the upper limit somewhat increases toward larger B/D ratios. In Figure 14 (*bottom*) the density parameter S_b is shown as a function of galaxy luminosity, normalized to Schechter's luminosity, showing that galaxy luminosity is not a dominant factor for the density contrast of a bar.

6.2. *Other Properties of the Bulges*

Sersic's (1968) law defined two parameters of the bulge, the effective radius r_e and the shape parameter n, which are shown as a function of B/D ratio for active and nonactive galaxies in Figure 15. These parameters are correlated with each other so that exponential bulges have smaller r_e than those approaching the $R^{1/4}$ density law. In addition, brighter bulges have larger r_e and n. On the other hand, r_e/h_r is similar for early- and late-type galaxies (see Table 7).

As expected, Seyfert galaxies and LINERs have B/D ratios typical for early-type galaxies. Since not all early-type galaxies are active, it is interesting to compare their properties: active early-type galaxies have marginally smaller r_e/h_r than their nonactive counterparts ($\langle r_e/h_r \rangle = 0.148 \pm 0.014$ vs. 0.161 ± 0.019, respectively), and the bulges are marginally more massive ($\langle B/D \rangle = 0.346 \pm 0.044$ vs. 0.268 ± 0.042), indicating that Seyfert galaxies and LINERs probably have more centrally concentrated bulges. However, the differences are marginal. In addition, the bright nuclei might affect the decomposition, so that this result should be verified by observations that are not seeing-limited and in which the nuclei are also modeled. For H II/starburst galaxies the effective radii of the bulges are clearly smaller than in the late-type galaxies in general ($\langle r_e/h_r \rangle = 0.104 \pm 0.016$ vs. 0.166 ± 0.019, respectively), although their B/D ratios are typical for late-type systems. The difference is statistically significant. This most possibly means that the bulges in H II/starburst galaxies are more centrally concentrated than in average late-type spirals, but again, the same caution as was made for Seyfert galaxies and LINERs is also valid here.

In the plane, most galaxies have either a thin bar (late-type spirals) or a thick bar (early-type galaxies), but there are also galaxies with a thick inner section with thin outer ends. These two-component bars were also noted by Block et al. (2001) and were interpreted in terms of a two-stage process of bar formation. We identified the clearest cases of this kind of system in our sample, shown in Table 8. Interestingly, except for one galaxy, they all show Seyfert- or LINER-type nuclear activity and have early Hubble types ($\langle T \rangle = 2.1$). In comparison to average early-type galaxies, these systems have marginally less massive bulges ($B/D = 0.221 \pm 0.037$ vs. 0.278 ± 0.070) and stronger perturbation strengths ($\langle Q_g \rangle = 0.352 \pm 0.049$ vs. 0.232 ± 0.017). However, the most outstanding property of these galaxies is that their bars are extremely massive: $\langle A_2 \rangle = 0.790 \pm 0.069$ in comparison to 0.580 ± 0.034, which is the mean for the early-type galaxies. In addition, the $m = 4$ amplitudes of the bars are more pronounced than in

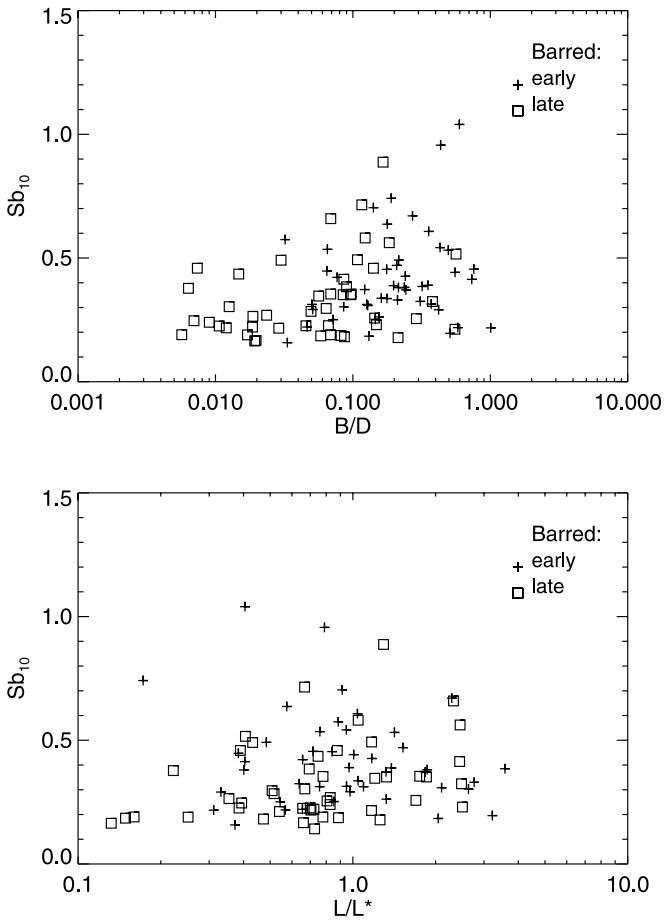

FIG. 14.—Same as Fig. 12, but instead of the density contrast parameter A_2, the parameter S_b, following Athanassoula (2003), is shown. The definition of the parameter is explained in the text.

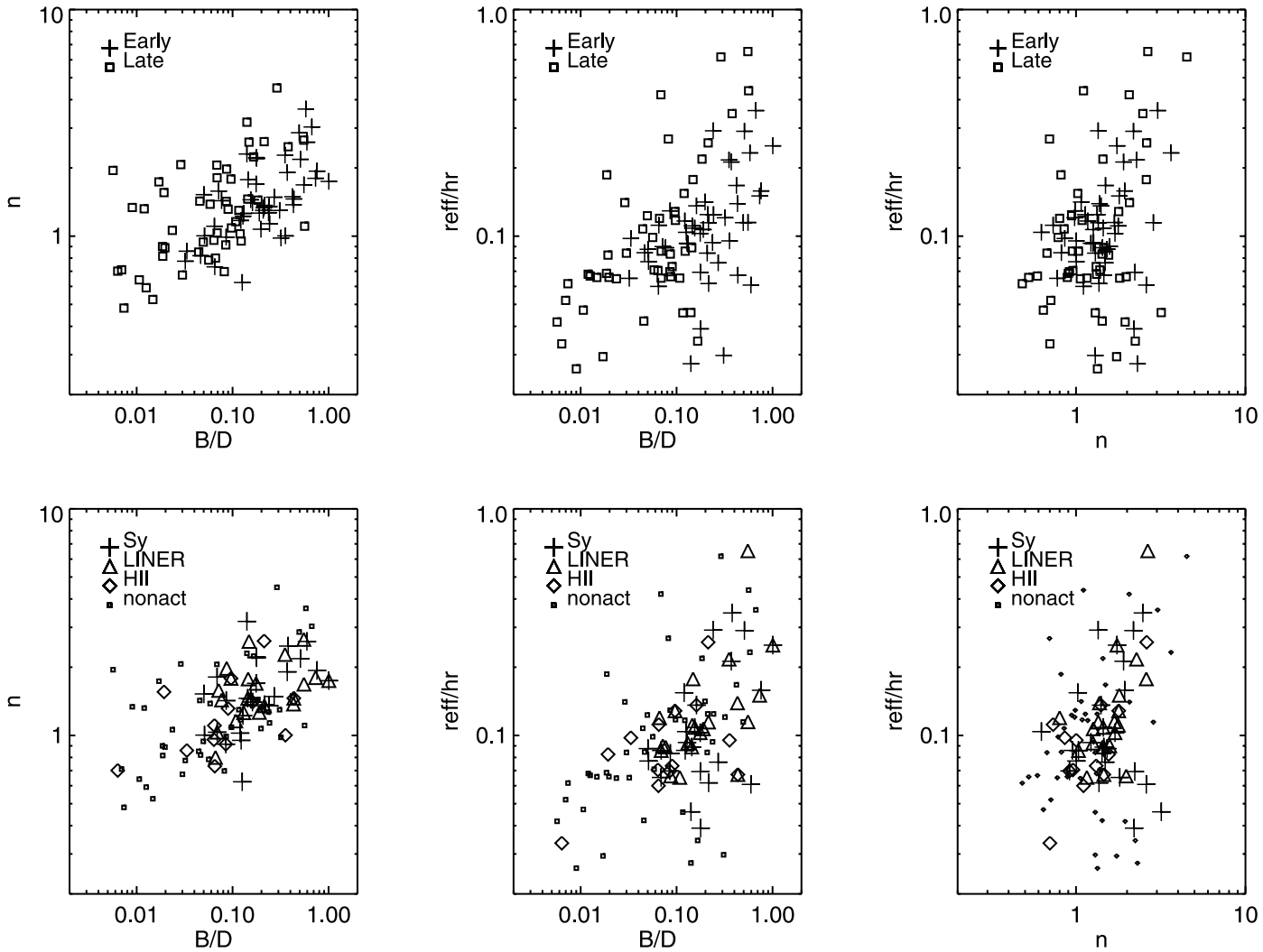

FIG. 15.—*Left panels*: Shape parameter n in Sérsic's (1968) law for the surface density distribution of galaxies vs. B/D ratio. *Middle panels*: Effective radius of the bulge scaled to the scale length of the disk (r_e/h_r) vs. B/D ratio. *Right panels*: Effective radius of the bulge vs. the shape parameter of the bulge. The top panels show the correlations for early- and late-type galaxies, whereas the bottom panels show the active and nonactive galaxies.

TABLE 7

MEAN EFFECTIVE RADIUS AND B/D RATIO

Sample	$\langle r_e/h_r \rangle \pm$ Mean Error	$\langle B/D \rangle \pm$ Mean Error	N
All	0.163 ± 0.011	0.209 ± 0.019	167
Sy	0.153 ± 0.017	0.306 ± 0.049	40
LINER	0.169 ± 0.022	0.349 ± 0.051	38
H II/starburst	0.104 ± 0.016	0.134 ± 0.027	22
Early ($T = 0$–3)	0.153 ± 0.011	0.317 ± 0.032	73
Late ($T = 4$–9)	0.166 ± 0.019	0.111 ± 0.014	89
Active, early (Sy+LINER+H II)	0.148 ± 0.014	0.346 ± 0.044	46
Active, early (Sy+LINER)	0.153 ± 0.016	0.367 ± 0.047	42
Nonactive, early	0.161 ± 0.019	0.268 ± 0.042	27
Active, late (Sy+LINER+H II)	0.149 ± 0.024	0.137 ± 0.024	31
Active, late (Sy+LINER)	0.148 ± 0.032	0.113 ± 0.059	23
Nonactive, late	0.175 ± 0.026	0.096 ± 0.017	58
Region I	0.130 ± 0.015	0.182 ± 0.020	64
Region II	0.141 ± 0.064	0.104 ± 0.044	17

TABLE 8
GALAXIES WITH THIN AND THICK BARS

Galaxy	Activity Type	Q_g	r_{Q_g}/h_r	B/D	A_2	A_4
NGC 2566	Nonactive	0.316	0.603	0.141	0.864	0.391
NGC 3227	Sy 1.5	0.158	2.123	0.177	0.444	0.272
NGC 4314	LINER	0.442	1.028	0.190	0.895	0.571
NGC 4548	LINER/Sy	0.344	0.932	0.176	0.723	0.337
NGC 4569	LINER/Sy	0.175	1.024	0.143	0.434	0.188
NGC 4593	Sy1	0.309	0.804	0.271	0.764	0.367
NGC 4643	LINER	0.251	0.943	0.431	0.828	0.516
NGC 7479	LINER/Sy2	0.696	1.099	0.069	0.867	0.555
NGC 7552	H II/LINER	0.395	0.766	0.435	1.148	0.724
NGC 7582	Sy2	0.436	1.259	0.178	0.932	0.551

bars of early-type galaxies in general ($A_2/A_4 = 1.8$ vs. 2.2, respectively).

7. Q_g-r_{Q_g}/h_r PLANE

In order to address the properties of bars more clearly, we show the barred galaxies in the Q_g-r_{Q_g}/h_r plane. A large majority of both early- and late-type galaxies appear in a rather narrow region, where Q_g steadily increases with increasing r_{Q_g}/h_r (Fig. 16, *top*). However, there are also many late-type galaxies that lie below this region and a few early-type systems that appear above the main body of the galaxies in the diagram. There is a tight correlation of Q_g with r_{Q_g}/h_r for most of the barred active galaxies, including Seyfert galaxies, LINERs, and H II/starburst galaxies (region I in Fig. 16, *bottom*). It is also obvious that the strongest bars in the diagram are nonactive or rarely show H II/starburst–like nuclear activity (region II): because of the lack of dilution by massive bulges, the gravitational perturbation strengths can be prominent. A few galaxies with bars with effectively very weak perturbation strengths near the nucleus (small Q_g and large r_{Q_g}/h_r) appear on top of the diagram and show Seyfert- or LINER-type nuclear activity.

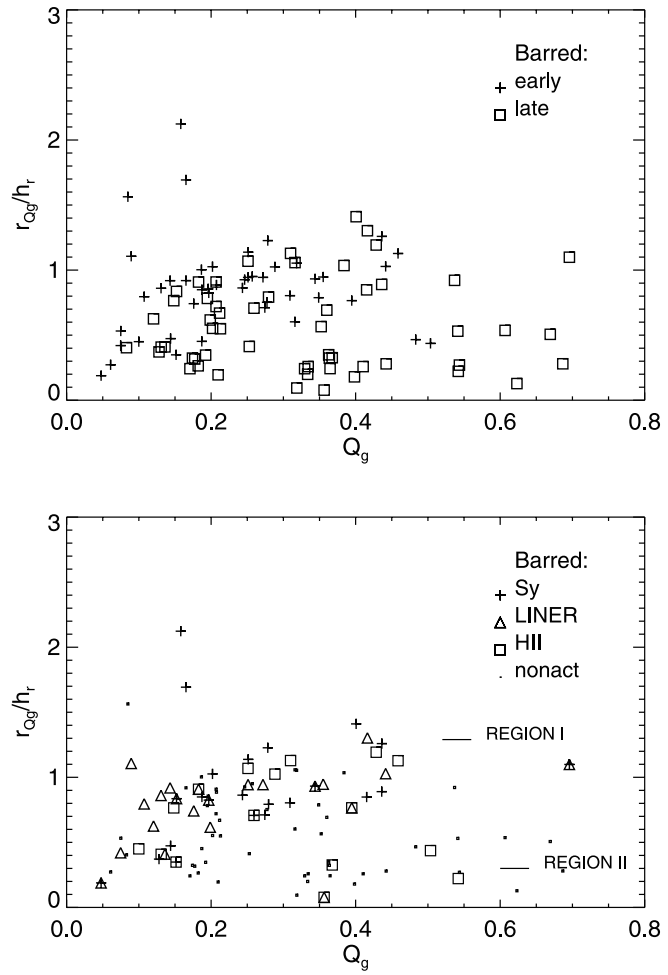

FIG. 16.—Distance of the maximum Q_T scaled to the scale length of the disk (r_{Q_g}/h_r) vs. the gravitational torque Q_g. *Top*: Barred early- and late-type galaxies. *Bottom*: Barred active and nonactive galaxies.

In Figure 17 we display Q_g and r_{Q_g}/h_r vs. the B/D ratio for the galaxies in the regions I and II. As expected for their late morphological types ($\langle T \rangle = 5.4$), galaxies in region II generally have small bulges ($B/D < 0.015$) or have no detectable bulge at all (six galaxies). There is one exception, NGC 1385, which has a larger B/D ratio. This galaxy has a bright exponential disk underlying the bulge and a prominent bar, and the density contrast between the bulge and the central parts of the disk is not very high, although enough to have a good fit in the decomposition. In spite of that, it is still possible that the uncertainty in the B/D ratio is large for this galaxy. As shown in Figure 18, the galaxies in region II have both prominent perturbation strengths and strong $m = 2$ amplitudes of density, indicating that the bars are genuinely strong, not solely because of the lack of dilution by massive bulges. Bars in these galaxies also have much smaller r_{Q_g}/h_r and $r_{Q_g}/r_{\rm bar}$-values than expected for their morphological types (see Tables 4 and 5).

In Figures 19*a*–19*d* we show all barred galaxies in the Q_g-r_{Q_g}/h_r plane, divided into active/nonactive early-type and active/nonactive late-type galaxies. By eye it is difficult to see any obvious characteristics that distinguish the active from the nonactive systems. In addition, active and nonactive early-type galaxies appear in a similar region in the Q_g-r_{Q_g}/h_r plane. However, nuclear activity does not appear in those late-type galaxies with effectively strong perturbation strengths near the nucleus, as was also shown in Figure 16. These galaxies are probably more irregular and lack prominent grand-design spiral arms, compared to the other galaxies in the sample. It also seems that bars in early-type galaxies have bright spots at the ends of the bars more often than bars in late-type systems, but this seems not to be related to nuclear activity.

8. DISCUSSION

Seyfert-type nuclear activity is generally attributed to supermassive black holes and the surrounding accretion disks, mainly because most of them exhibit strong 2–10 keV X-ray

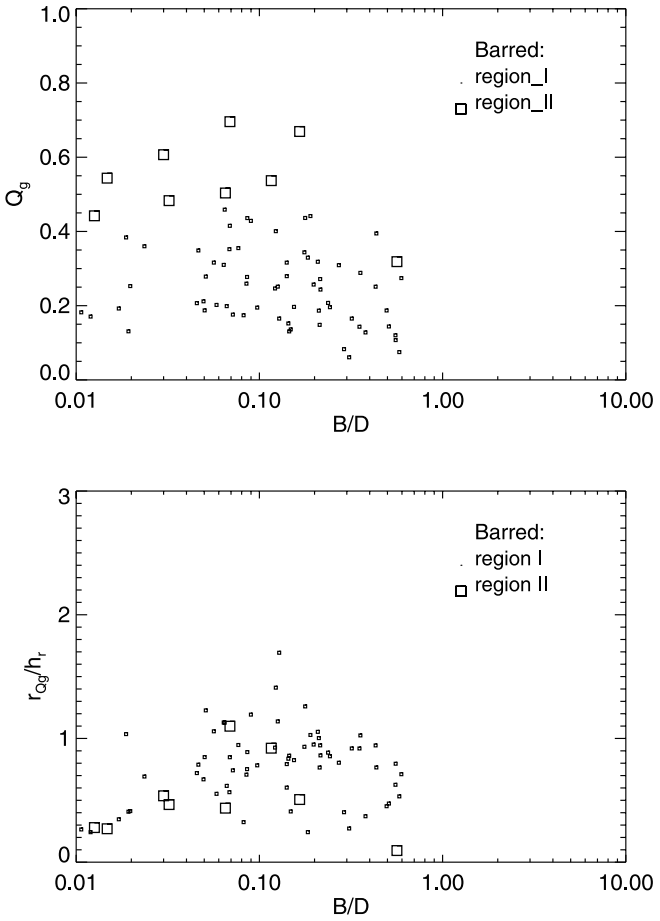

FIG. 17.—*Top*: Maximum relative gravitational torque Q_g vs. B/D ratio for the two regions as defined in Fig. 15. *Bottom*: Distance of the maximum Q_T scaled to the scale length of the disk (r_{Q_g}/h_r) vs. B/D ratio for the same galaxies.

luminosities, particularly in type 1 Seyfert galaxies. On the other hand, LINERs also have prominent low-ionization emission lines, which suggests that other mechanisms, such as shocks in the surrounding interstellar medium or stellar photoionization, might also explain their nuclear activity. Although the origin of LINERs is not settled, photoionization by a nonstellar continuum seems to be a plausible explanation, especially for LINERs in early-type galaxies. In such galaxies, although their off-nuclear regions can have prominent shocks, the nuclei emit strong, hard X-ray emission, which can be produced only by powerful black holes. In many statistical studies of bar fractions, both Seyfert galaxies and LINERs are considered to be real AGNs, which therefore seems to have a justification. However, it has also been suggested that near-nuclear star formation and AGNs might be intimately related, which was first suggested for high-redshift galaxies by Sanders et al. (1988), supposing that galaxies with strong starbursts detected as ultraluminous infrared galaxies were predecessors of AGNs, in a phase of galaxy evolution in which the AGNs still reside in dusty circumnuclear regions. In the same line with this picture, optical and IR emission lines in LINERs at low redshifts can be understood as aging starbursts, which might be the case especially in LINERs appearing in late-type spirals. When an H II region becomes older, supernovae are born, causing shock excitation in the interstellar medium, possibly ending with a supernova-like shock-excited spectrum (Alonso-Herrero et al. 2000). Therefore, any differences in Seyfert, LINER, and H II/starburst galaxies would be interesting.

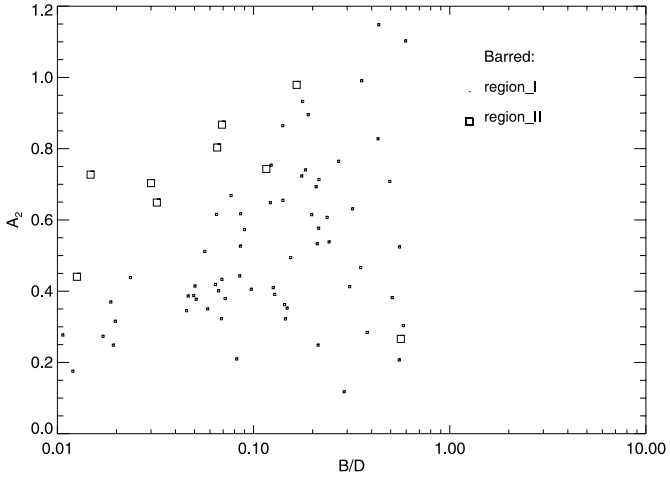

FIG. 18.—Plot of the $m = 2$ amplitude of density A_2 vs. B/D ratio for the galaxies as defined in the two regions in Fig. 15

Before discussing the properties of bars in different activity types, we may ask whether bars really play an important role for the AGNs. If they do, one would expect to see bars more frequently in AGNs than in nonactive systems, for which controversial results appear in the literature. In comparison to many other studies, the advantage of our sample is that, being magnitude-limited, the samples of AGNs and nonactive galaxies are selected in a similar manner. In addition, bar identifications exist in both the optical and the near-IR for the same galaxies, made by the same person, thus making possible a fair comparison of bar fractions in the optical and in the near-IR. We found that the result depends critically on the method and wavelength used to identify bars. In the near-IR, where most of the emission from stellar mass resides, Seyfert galaxies, LINERs, and H II/starburst galaxies were found to have SB-type bars or Fourier bars more frequently than nonactive systems, which indicates that bars most probably play some role in the process of fueling not only H II/starburst galaxies but also Seyfert- and LINER-type nuclear activity. We also found that in the optical region, a larger fraction of bars are obscured by dust in LINERs than in Seyfert galaxies (34% vs. 13%), which hints at the existence of a large amount of dust and probably also strong, ongoing nuclear/circumnuclear star formation in LINERs.

However, it is not clear whether this also means that bars trigger/fuel AGNs. It may still be possible that bars transfer gas to the 100 pc scale in galaxies, which then either causes a circumnuclear starburst or partly obscures the broad-line region in AGNs, as suggested by Maiolino, Risaliti, & Salvati (1999). They found that even 80% of Compton-thick, type 2 Seyfert galaxies are barred. An interesting point of comparison is giant low-surface brightness galaxies, which have AGNs as frequently as the high surface brightness galaxies, although they have much lower bar fractions (Sprayberry et al. 1998): the fraction of Seyfert galaxies and LINERs in both our study and the study by Sprayberry et al. is 35%–37%. On the other hand, giant high and low surface brightness galaxies have similar bulges (Sprayberry et al.), which seem to be important for the onset of nuclear activity. Low surface brightness galaxies might have mechanisms other than bars, such as weak galaxy interactions, that may induce gas inflows to the central regions of the galaxies.

One would also expect to see some characteristic, such as the strength of a bar, which controls the fueling of the active

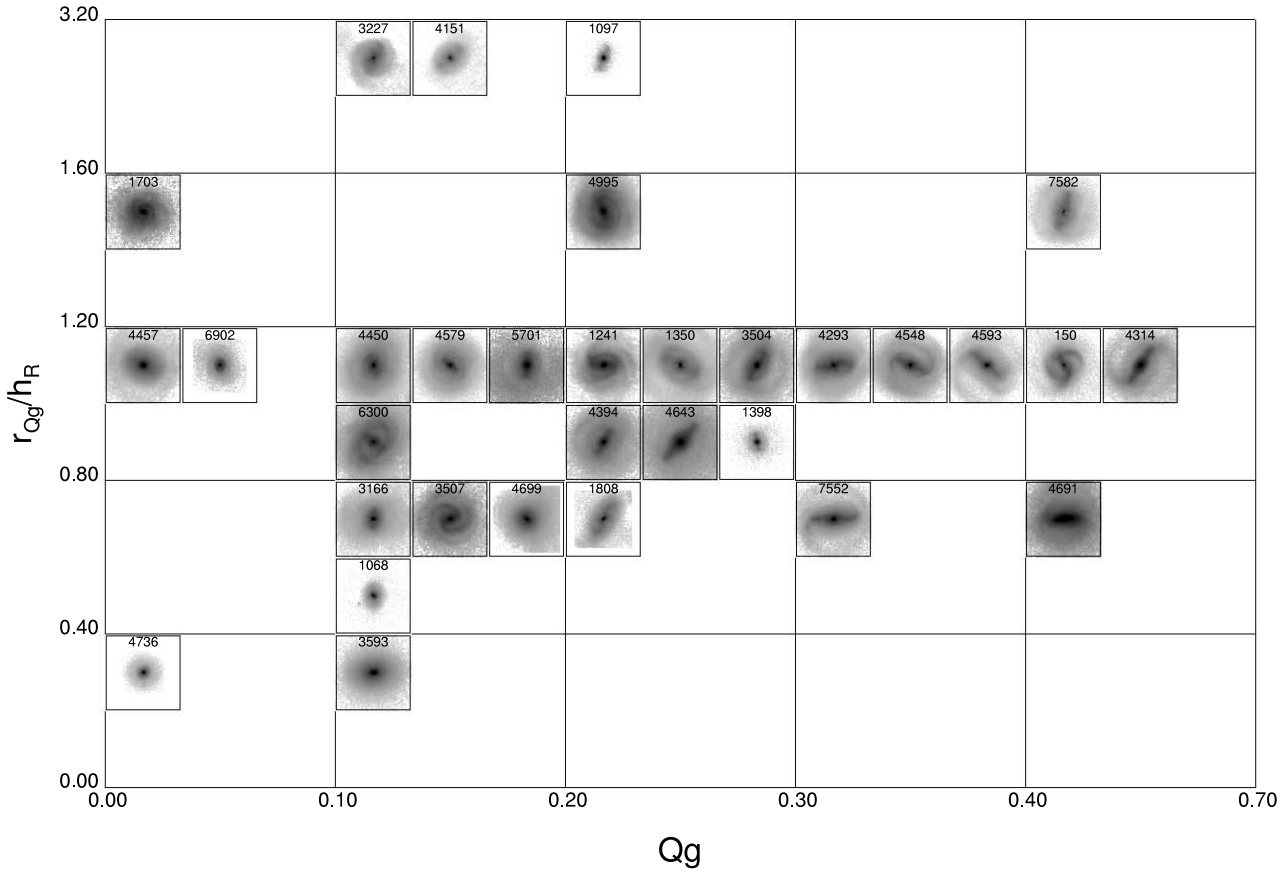

FIG. 19*a*

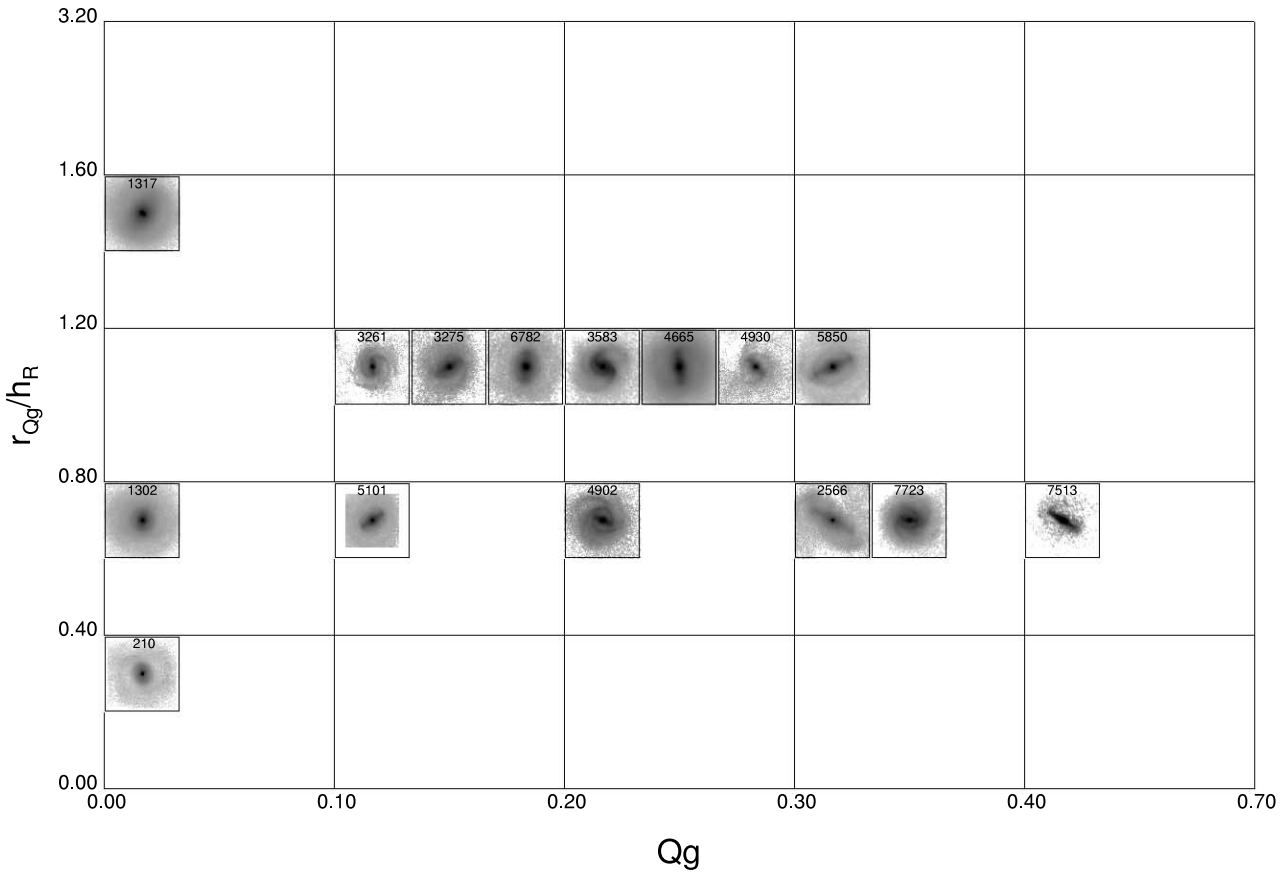

FIG. 19*b*

FIG. 19.—Deprojected images for barred galaxies shown in the Q_g-r_{Q_g}/h_r plane. Separately shown are (*a*) the active early-type, (*b*) nonactive early-type, (*c*) active late-type, and (*d*) nonactive late-type galaxies. In each case, the width of the frame corresponds to $2R_{\rm opt}$.

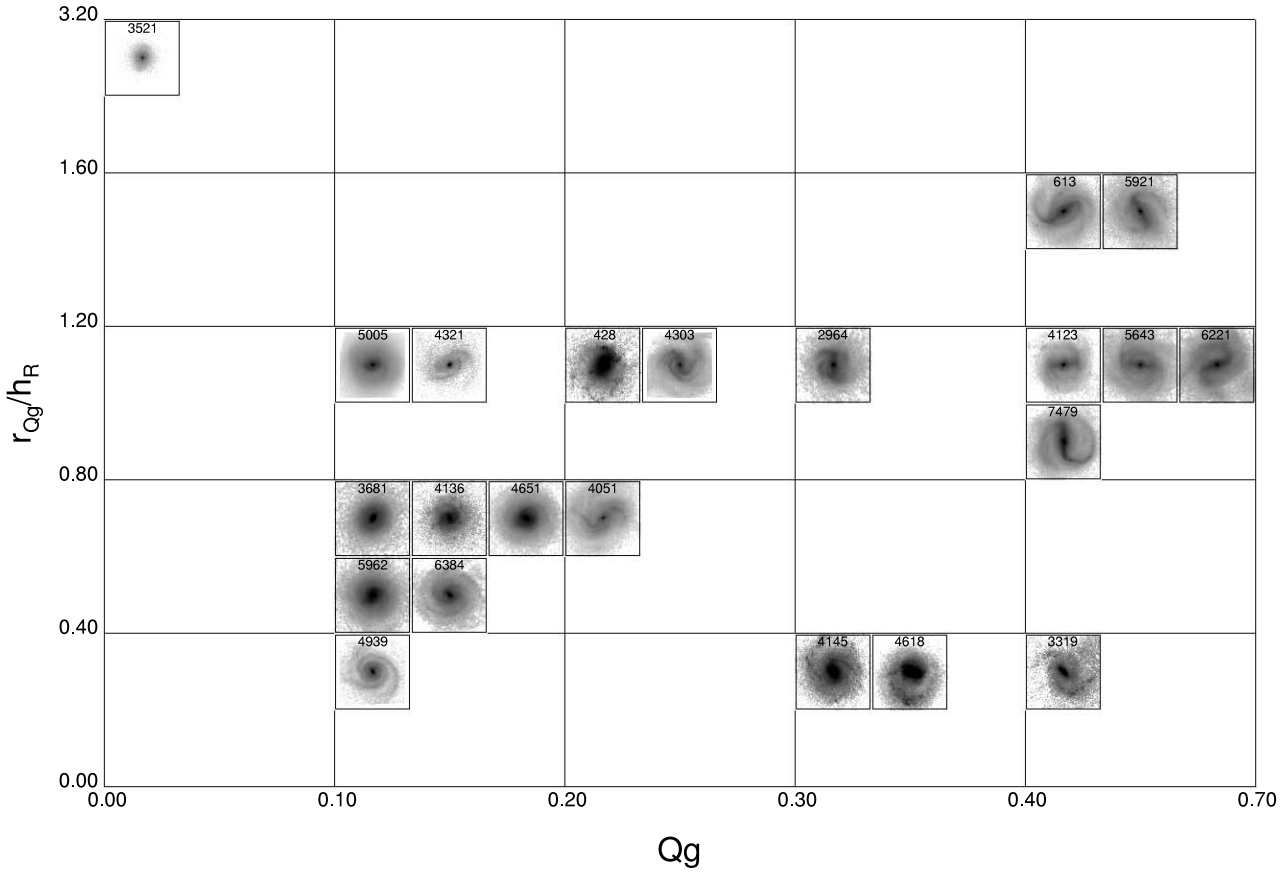

FIG. 19*c*

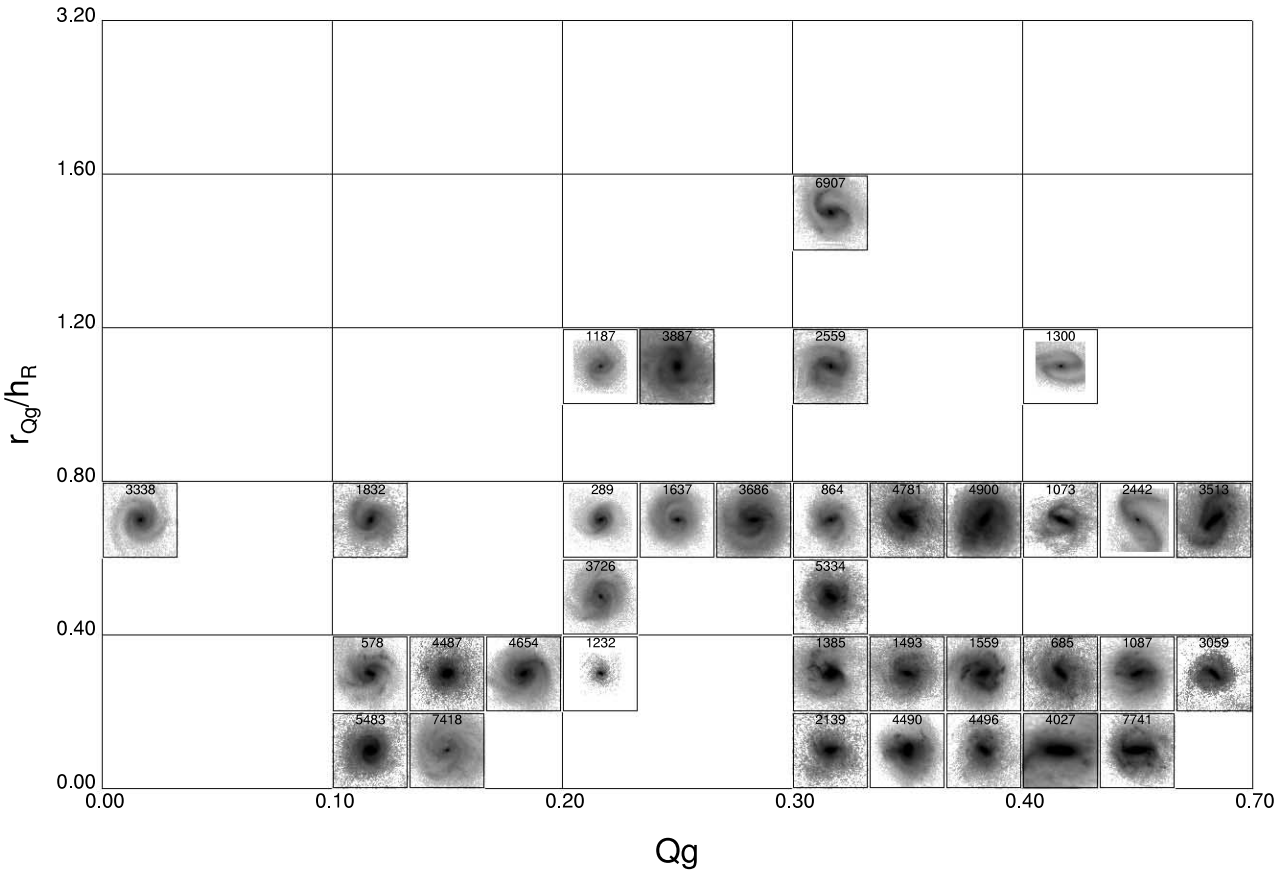

FIG. 19*d*

FIG. 19.—*Continued*

nucleus, to be different between active and nonactive galaxies. In this study bars in active galaxies were found to be in many respects similar to bars in the nonactive systems of similar morphological types. In particular, the small perturbation strengths in Seyfert galaxies and LINERs, suggested by LSR02 based on a smaller 2MASS sample, can now be completely explained by the dilution induced by massive bulges, an effect that is more prominent for early-type galaxies. However, there are also some characteristics of bars that are different in active and nonactive systems: for example, the distances of the maximal tangential forces in Seyfert galaxies and LINERs appear on the average more toward the edge of the bar ($r_{Q_g}/r_{\rm bar}$ is larger) than in the nonactive galaxies of similar Hubble types. This probably means that the mass distributions of bars in Seyfert galaxies and LINERs are flatter than in their nonactive counterparts. Active galaxies might also have more compact bulges than nonactive systems, but that should be verified by higher resolution observations and after applying methods that better take into account the nuclei. It also seems that some minimum mass of the bulge ($B/D > 0.05$) is required for the onset of Seyfert- and LINER-type nuclear activity, probably indicating that pre-existing black holes reside in the centers of the massive bulges. Black holes are also expected to be more massive in early-type galaxies, which explains why Seyfert galaxies and LINERs appear mostly in early-type galaxies.

We next discuss how well the bulges can explain the observed properties of bars in early- and late-type galaxies and in active and nonactive systems, based on the dynamical models of Athanassoula (2003). Her models predict that when galaxies evolve in time, the properties of bars are modified by the interaction between the disk and the bulge/halo. According to her models, a massive bulge or a cold dark matter halo can absorb the angular momentum emitted by the bar, with the consequence that the bar pattern speed slows down, thus increasing the corotation radius of the bar, leading also to the lengthening of the bar. At the same time, the bar becomes thinner and the density contrast with the underlying disk increases, which according to Athanassoula also means that the bar becomes stronger. Therefore, in her models bars in halo- or bulge-dominated disks are stronger than those grown in disk-dominated surroundings. More centrally peaked spheroids lead to bars that are longer and thinner, have flatter surface densities, and also have more pronounced peanut structures and rectangular-like isodensities, especially in the outer parts of the bars.

We confirm the previous observations showing that bars are longer in early-type galaxies than in late-type systems (Elmegreen & Elmegreen 1985), but the length of a bar is only weakly correlated with the relative mass of the bulge: bars are on the average shorter only in the disk-dominated, late-type galaxies with $B/D < 0.05$, whereas in the galaxies with more massive bulges, the length of a bar is independent of the B/D ratio. The maximum value of the density contrast, using both A_2 and S_b, slightly increases toward larger relative bulge masses, which is in the same line with the model predictions, but the tendency is weak. More importantly, we find that if bars are long and have strong density contrasts, it does *not* mean that the bars also have strong perturbation strengths. Since we have also shown (LSR02, BLS04) that the perturbation strength is correlated with the ellipticity of a bar, our results contradict the model predictions by Athanassoula (2003). Since Seyfert galaxies and LINERs appear preferentially in early-type galaxies, the same argument is largely valid also for them. We also showed that bars in active galaxies probably have flatter surface brightness distributions than in nonactive systems, which on the bases of Athanassoula's models could be understood if these galaxies had more centrally concentrated bulges.

Galaxies in region II in the Q_g-r_{Q_g} plane form an interesting subgroup, which is also difficult to understand in the framework of the above discussed models. These galaxies have smaller bulges than the late-type galaxies in general in our sample, and the bars are also more massive and have considerably stronger perturbation strengths than bars in late-type galaxies in general. These bars are so prominent that the strengths cannot be explained solely by the lack of dilution by massive bulges. Bars in these galaxies have totally different mass distributions from those in late-type galaxies in general, being more centrally concentrated (small $r_{Q_g}/r_{\rm bar}$). According to the models of Athanassoula (2003), massive central halos can absorb the angular momentum of a bar, which would be a reasonable explanation for the large bars if these galaxies had halos as massive as halos in typical late-type dwarf galaxies (Persic et al. 1996). However, the galaxies in region II have absolute brightnesses similar to those of late-type galaxies in general ($M_B = -19.8$ vs. -19.9, respectively). Therefore, bars in these galaxies are probably formed by some mechanism other than that of most of the bars in our sample, or alternatively, they represent some earlier phase in galaxy evolution. These galaxies are particularly interesting, because they never show Seyfert- or LINER-type nuclear activity and in only a few cases have an H II/starburst nucleus.

In order to understand the present observations of bars, a more comprehensive picture of galaxy evolution is needed, in which the secular evolution manifests itself in a more complicated manner than in the evolutionary scenario outlined by Athanassoula (2003), or in which galaxy interactions are also taken into account. For example, Noguchi (1996) has suggested that galaxy interactions could play an important role in the formation of bars, or that bars in Hubble types later than Scd are formed from central concentrations of the disk matter created by clumpy driven inflow (Noguchi 2000). In this case the central mass component evolves to an axisymmetric bulge instead of forming a real bar. Some dynamical models (Berentzen et al. 2003) also predict that galaxy interactions might accelerate the transition from a strongly barred galaxy to a weakly or nonbarred galaxy.

9. CONCLUSIONS

We have used a sample of 158 galaxies from the Ohio State University Bright Galaxy Survey, extended by 22 galaxies from the Two Micron All Sky Survey (OSUBGS+2MASS), to study bar fractions and gravitational perturbation strengths in active and nonactive galaxies. Galaxy classifications by EFP02 made in both the B and H bands have allowed a fair comparison of bar fractions in the optical and in the near-IR and have also allowed us to evaluate the reasons for the previous controversial results in the literature. Bar fractions were also estimated using a Fourier approach to identify bars.

Gravitational perturbation strengths Q_g were calculated using a polar grid method inferring the gravitational potentials from H-band images under the assumption of a constant mass-to-luminosity ratio and an exponential vertical density law. Two-dimensional bulge-disk-bar decomposition was used to eliminate the impact of the bulge deprojection stretch on the calculated forces. The radial scale lengths h_r were derived from the decomposition, and they were used to estimate the vertical scale heights h_z based on the empirical correlation

between h_r and h_z (de Grijs 1998). In order to evaluate the impact of the bulges on the properties of the bars, bulge-disk-bar decomposition was used to calculate B/D luminosity ratios of the same galaxies.

The main results are the following:

1. In the near-IR, Seyfert galaxies, LINERs, and H II/starburst galaxies were found to have similar fractions of Fourier bars (71% ± 10%, 72% ± 7%, and 67% ± 8%, respectively, or SB-type bars), which is more than in the nonactive galaxies (55% ± 5%), but if SAB-type bars are also included, as much as 95% ± 5% of the H II/starburst galaxies have bars. In the optical region, H II/starburst galaxies were found to have bars marginally more frequently than Seyfert galaxies or nonactive galaxies (78% ± 9%, 62% ± 9%, and 57% ± 5%, respectively). In addition, in comparison to Seyfert galaxies, in the optical region a significantly larger number of bars were obscured by dust in LINERs (34% vs. 13%).

2. We found that bars in the early-type galaxies are on the average *longer* and *more massive* (have large A_2 amplitudes of density) and have *weaker* perturbation strengths (Q_g) than bars in the late-type systems, which means that the properties of bars cannot be explained solely by the time evolutionary picture of bars as outlined by Athanassoula (2003). In addition, Q_g increases with increasing A_2, but the correlation is more shallow for the early-type galaxies.

3. Bars in Seyfert galaxies and LINERs have weaker perturbation strengths (Q_g) than bars in H II/starburst galaxies or in nonactive systems, which is in accordance with their Hubble type. This is in agreement with the previous result by LSR02, who found that bars are weaker in active than in nonactive systems, but now it is clear that Q_g is closely related to the Hubble type. We also found a small difference in the properties of bars between active and nonactive galaxies within one Hubble type: namely, in early-type galaxies bars were found to be longer and flatter (larger $r_{Q_g}/r_{\rm bar}$) for Seyfert galaxies and LINERs than for their nonactive counterparts.

4. Massive bulges were found to be important in controlling the perturbation strengths: for $B/D = 0 \rightarrow 1$, Q_g can be diluted by a factor of 0.1–0.6, corresponding to five bar torque classes as defined BB01. However, the bulges are less important for the lengths and masses of the bars. The length of a bar as a function of the B/D ratio is nearly constant for early-type galaxies and also depends very little on the B/D ratio for the late-type systems.

5. The masses and lengths of the bars for Seyfert galaxies, LINERs, and H II/starburst galaxies are correlated with the B/D ratio in a manner rather similar to that for the early-type galaxies. In addition, a minimum B/D ratio of 0.05 was found for Seyfert- and LINER-type nuclear activity.

6. A group of late-type galaxies with atypical barred properties was identified. Bars in these galaxies are massive (large A_2), the perturbation strengths (Q_g) are extremely strong, and the mass distributions of the bars are centrally peaked ($r_{Q_g}/r_{\rm bar}$ is small). The bulges of these galaxies are small, but that is not the only reason for the strong perturbation strengths. These galaxies are not expected to have exceptionally massive halos, because they have luminosities similar to those of late-type galaxies in general. Interestingly, these galaxies are largely nonactive and only rarely show H II/starburst–type nuclear activity.

7. Some of the galaxies have a thick inner section with thin outer ends. These galaxies have early Hubble types and, except for one galaxy, show Seyfert- or LINER-type nuclear activity. In comparison to bars in early-type galaxies in general, bars in these galaxies are remarkably massive ($A_2 = 0.790$ vs. 0.574, respectively). In addition, the masses of their bulges are marginally smaller, and the perturbation strengths marginally larger, than in the early-type galaxies in general.

E. L. and H. S. acknowledge the support of the Academy of Finland, and E. L. also of the Magnus Ehrnrooth Foundation. R. B. acknowledges the support of National Science Foundation (NSF) grant AST 02-05143 to the University of Alabama. Funding for the OSUBGS was provided by grants from the NSF (grants AST 92-17716 and AST 96-17006), with additional funding from the Ohio State University. This publication also utilized images from 2MASS, which is a joint project of the University of Massachusetts and the Infrared Processing and Analysis Center of the California Institute of Technology, funded by the National Aeronautics and Space Administration and NSF. This research has also made use of the NED, which is operated by the Jet Propulsion Laboratory, California Institute of Technology, under contract with the National Aeronautics and Space Administration. We also thank the anonymous referee for valuable comments that improved the quality of the paper.

REFERENCES

Alonso-Herrero, A., Rieke, M. J., Rieke, G. H., & Shields, J. C. 2000, ApJ, 530, 688
Athanassoula, E. 1992, MNRAS, 259, 345
———. 2003, MNRAS, 341, 1179
———. 2004, in Galaxies and Chaos, ed. G. Contopolous & N. Voglis (Berlin: Springer), in press (astro-ph/0302521)
Berentzen, I., Athanassoula, E., Heller, C. H., & Fricke, K. J. 2003, MNRAS, 341, 343
Block, D. L., Bournaud, F., Combes, F., Puerari, I., & Buta, R. 2002, A&A, 394, L35
Block, D. L., Puerari, I., Knapen, J. H., Elmegreen, B. G., Buta, R., Stedman, S., & Elmegreen, D. M. 2001, A&A, 375, 761
Boker, T., Stanek, R., & Marel, R. P. 2003, AJ, 125, 1073
Bournaud, F., & Combes, F. 2002, A&A, 392, 83
Bureau, M., & Freeman, K. C. 1999, AJ, 118, 126
Buta, R., & Block, D. 2001, ApJ, 550, 243 (BB01)
Buta, R., Block, D. L., & Knapen, J. H. 2003, AJ, 126, 1148
Buta, R., & Combes, F. 1996, Fundam. Cosmic Phys., 17, 95
Buta, R., Laurikainen, E., & Salo, H. 2004, AJ, 127, 279 (BLS04)
Buta, R., Mitra, S., Corwin, H. G., & de Vaucouleurs, G. 1994, AJ, 107, 118
Carollo, C. M., Stiavelli, M., de Zeeuw, P. T., & Mack, J. 1997, AJ, 114, 2366
Carollo, C. M., Stiavelli, M., & Mack, J. 1998, AJ, 116, 68
Combes, F., Debbasch, F., Friedli, D., & Pfenniger, D. 1990, A&A, 233, 82
Combes, F., & Sanders, R. H. 1981, A&A, 96, 164
de Grijs, R. 1998, MNRAS, 299, 595
de Vaucouleurs, G., & Buta, R. 1983, AJ, 88, 939
de Vaucouleurs, G., de Vaucouleurs, A., & Buta, R. 1981, AJ, 86, 1429
de Vaucouleurs, G., de Vaucouleurs, A., Corwin, H. G., Jr., Buta, R., Paturel, G., & Fouque, P. 1991, Third Reference Catalogue of Bright Galaxies (New York: Springer) (RC3)
Elmegreen, B. G., & Elmegreen, D. 1985, ApJ, 288, 438
Englmaier, P., & Gerhard, O. 1997, MNRAS, 287, 57
Englmaier, P., & Shlosman, I. 2000, ApJ, 528, 677
Eskridge, P. B., et al. 2000, AJ, 119, 536
———. 2002, ApJS, 143, 73 (EFP02)
Fabian, A. C. 1999, MNRAS, 308, L39
Graham, A. W. 2001, AJ, 121, 820
Haehnelt, M. G., Natarajan, P., & Rees, M. J. 1998, MNRAS, 300, 817
Ho, L. C., Filippenko, A. V., & Sargent, W. L. W. 1997, ApJ, 487, 591
Hunt, L. K., & Malkan, M. A. 1999, ApJ, 516, 660
Knapen, J. H., Shlosman, I., & Peletier, R. 2000, ApJ, 529, 93 (KSP00)
Laine, S., Knapen, J. H., Perez-Ramirez, D., Doyon, R., & Nadeau, D. 1999, MNRAS, 302, L33

Laine, S., Shlosman, I., Knapen, J. H., & Peletier, R. F. 2002, ApJ, 567, 97 (LSKP02)
Laurikainen, E., & Salo, H. 2002, MNRAS, 337, 1118 (LS02)
Laurikainen, E., Salo, H., & Rautiainen, P. 2002, MNRAS, 331, 880 (LSR02)
Lutticke, R., Dettmar, R. J., & Pohlen M. 2000, A&A, 362, 435
Magorrian, J., et al. 1998, AJ, 115, 2285
Maiolino, R., Risaliti, G., & Salvati, M. 1999, A&A, 341, L35
Malkan, M. A., Gorjian, V., & Tam, R. 1998, ApJS, 117, 25
Marquez, I., et al. 2000, A&A, 360, 431
Martin, P. 1995, AJ, 109, 2428
Martinet, L., & Friedli, D. 1997, A&A, 323, 363
Martini, P., & Pogge, R. W. 1999, AJ, 118, 2646
Mathur, S. 2000, MNRAS, 314, L17
McLeod, K. K., & Rieke, G. H. 1995, ApJ, 441, 96
Merritt, D., & Ferrarese, L. 2001, MNRAS, 320, L30
Möllenhoff, C., & Heidt, J. 2001, A&A, 368, 16
Moles, M., Marquez, I., & Perez, E. 1995, ApJ, 438, 604
Mulchaey, J. S., & Regan, M. W. 1997, ApJ, 482, L135 (MR97)
Noguchi, M. 1996, ApJ, 469, 605
———. 2000, MNRAS, 312, 194
Patsis, P. A., & Athanassoula, E. 2000, A&A, 358, 45
Persic, M., Salucci, P., & Stel, F. 1996, MNRAS, 281, 27
Pfenniger, D., & Friedli, D. 1991, A&A, 252, 75
Pfenniger, D., & Norman, C. 1990, ApJ, 363, 391
Quillen, A. C. 2002, AJ, 124, 722
Quillen, A. C., Frogel, J. A., & Gonzalez, R. A. 1994, ApJ, 437, 162
Quillen, A. C., Frogel, J. A., Kenney, J. D., Pogge, R. W., & Depoy, D. L. 1995, ApJ, 441, 549
Raha, N., Sellwood, J. A., James, R. A., & Kahn, F. D. 1991, Nature, 352, 411
Sandage, A., & Bedke, J. 1994, The Carnegie Atlas of Galaxies (Washington, DC: Carnegie Inst.)
Sandage, A., & Tammann, G. 1981, The Revised Shapley-Ames Catalog of Bright Galaxies (Washington, DC: Carnegie Inst.)
Sanders, D. B., Soifer, B. T., Elias, J. H., Madore, B. F., Matthews, K., Neugebauer, G., & Scoville, N. Z. 1988, ApJ, 325, 74
Sanders, R. H., & Tubbs, A. D. 1980, ApJ, 235, 803
Schlegel, D. J., Finkbeiner, D. P., & Davis, M. 1998, ApJ, 500, 525
Sellwood, J. A., & Wilkinson, A. 1993, Rep. Prog. Phys., 56, 173
Sérsic, J. L. 1968, Atlas de Galaxies Australes (Cordoda: Obs. Astron.)
Shlosman, I., Begelman, M., & Frank, J. 1990, Nature, 345, 679
Simkin, S. M., Su, H. J., & Schwarz, M. P. 1980, ApJ, 237, 404
Skrutskie, M. F., et al. 1997, in The Impact of Large-Scale Near-IR Surveys, ed. F. Grazon et al. (Dordrecht: Kluwer), 25
Sprayberry, D., Impey, C. D., Bothun, G. D., & Irwin, M. J. 1998, AJ, 116, 1650
Tully, R. B. 1988, Nearby Galaxies Catalogue (Cambridge: Cambridge Univ. Press)
Veilleux, S., & Osterbrock, D. E. 1987, ApJS, 63, 295